Regional Pole Placement Design Based Stabilization for Cart Inverted Pendulum System

A Thesis submitted in

May 2015

to the department of

Electrical Engineering

(Control & Automation)

of

National Institute Of Technology Rourkela

in partial fulfilment of the requirements for the degree of

Master of Technology

by

MARRAPU DEEPTHI

Roll no. 213EE3301

Under the Guidance of

Prof. Sandip Ghosh

Department of Electrical Engineering

National Institute Of Technology Rourkela

Rourkela, Odisha, 769008, India

May-2015

Dedicated to my family and

My friends

Department of Electrical Engineering
National Institute of Technology Rourkela
Rourkela-769008, Odisha, India.

Certificate

This is to certify that the work in the thesis entitled *Regional Pole Placement Design Based Stabilization for Cart Inverted Pendulum System* by ***Marrapu Deepthi*** is a record of an original research work carried out by her under my supervision and guidance in partial fulfilment of the requirements for the award of the degree of Master of Technology with the specialization of Control & Automation in the department of Electrical Engineering, National Institute of Technology Rourkela. Neither this thesis nor any part of it has been submitted for any degree or academic award elsewhere.

Place: NIT Rourkela
Date: May 2015

Prof. Sandip Ghosh
Dept. of Electrical Engineering
NIT Rourkela

ACKNOWLEDGEMENT

I am grateful to numerous local and global peers who have contributed towards shaping this thesis. At the outset, I would like to express my sincere thanks to Prof.Sandip Ghosh for his advice during my thesis work. As my supervisor, he has constantly encouraged me to remain focused on achieving my goal. His observations and comments helped me to establish the overall direction of the research and to move forward with investigation in depth. He has helped me greatly and been a source of knowledge.

I would like to thank Sudipto Chakaborthy for helping with the real time set up. I am really thankful to my all friends and especially Abhilash, Sowjanya, Anusha, Srikanya, Sudipta, Karmila, Abhishek, Pavan and Upasana. My sincere thanks to everyone who has provided me with kind words, a welcome ear, new ideas, useful criticism, or their invaluable time, I am truly indebted.

I must acknowledge the academic resources that I have got from NIT Rourkela. I would like to thank administrative and technical staff members of the Department who have been kind enough to advise and help in their respective roles.

Last, but not the least, I would like to dedicate this thesis to my family, for their love, patience, and understanding.

Marrapu Deepthi

213EE3301

ABSTRACT

The inverted pendulum has been considered as a benchmark control problem due to its nonlinearity and stabilization around the unstable equilibrium point. To achieve stabilization, it is well known that all the closed loop system poles should lie in left half of s-plane. In present work, different approaches have taken to shift the system poles to left half of the plane. At first Linear Quadratic Regulator (LQR) is used, where the desired pole locations can be achieved by suitably selecting weight matrix of cost function. With this guaranteed cost control scheme, one does not have to bother about specifying closed-loop poles. Next, a two loop PID is designed based on pole matching conditions. Where the closed loop with unknown controller coefficient characteristic equation is compared with desired characteristics, to find out the controller gains. In both the methods, one has to deal with point wise pole placing, which can be tricky sometimes. With the recent development of LMIs tool, regional pole placement is well suited to achieve the goal. At last, a regional pole placement controller is synthesized, where desired specifications are transformed into LMI regions. In present case, a conical sector of left half plane is taken so that stabilisation with better transient performance can be achieved.

Contents

Table of Contents

List of Figures

List of Tables

Nomenclature

Abbreviation	Description
CIPS	Cart-Inverted Pendulum System
SIMO	Single-Input-Multi-Output
IFAC	International Federation of Automatic Control
DC	Direct Current
LQR	Linear Quadratic Regulator
LMI	Linear Matrix Inequality
PID	Proportional Integral Derivative
DOF	Degrees Of Freedom
A/D	Analog-to-Digital
D/A	Digital-to-Analog
PI	Performance Index
RPP	Regional pole placement

CHAPTER 1

1. INTRODUCTION

Balancing a broom stick or a ruler on a palm in the desired upright position by moving the hand continuously is a most common play which almost everyone had tried in their childhood. The basic working of inverted pendulum is the same too. But the degree of freedom for the moment is limited only in one direction unlike your hand moment which is free to move in any direction. An inverted pendulum system thus like a broom stick is inherently unstable. An external force is necessary to keep the pendulum in upright position. So a proper control design is necessary to make the inverted pendulum stable.

This inverted pendulum is known since 1960's. It consists on a rod pivoted at one end and that pivot point is mounted on a cart which moves along a smooth track in one dimension under the influence of control input. The control task is to stabilize the pendulum in inverted position by applying this control force.

1.1 Applications of Inverted Pendulum

- Control of under-actuated robotic system:

Fig: 1.1(a) robotic system

Courtesy: www.reevoseek.com

Under-actuated systems are the systems having fewer actuators than the degree of freedom and are to be controlled. Inverted pendulum is one such typical system.

- Design of mobile inverted pendulum systems:

Mobile wheeled inverted pendulum is used for personal transportation like in Segway. Two wheeled motorized vehicle provide enhanced

Fig: 1.1(b) Segway

Courtesy: www.msu.edu

- Rocket launching:

Inverted pendulum dynamics represent rocket and missile launching system whose centre of drag is ahead of the centre of gravity which leads to aerodynamic instability

Fig: 1.1(c) rocket launching

Courtesy: hrdi.engin.umich.edu

- Model of human stand still:

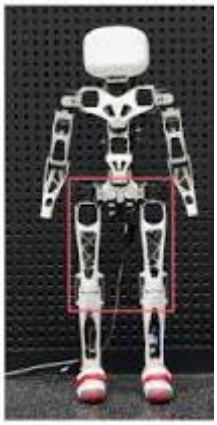

Inverted pendulum model represent human stand still position. The muscles and tissues are represented by the spring and damper which will be leading to a negative feedback loop that is required for the stabilisation of the inverted pendulum in the case when the springs are stiff enough

Fig: 1.1(d) human stand still model

Courtesy: flowers.inria.fr

Other applications include Building under action of earthquake, biped locomotion, model of human standstill, seismometers

1.2 Literature Review

Inverted pendulum has been an important benchmark problem in control systems for testing various controllers and in robotics since 1960's. The inverted pendulum was first used in the year 1844 in Great Britain in seismometer to detect the slightest vibrations. Later the applications of inverted pendulum dynamics had been wide spread as in [6] and hence gained its popularity.

LQR has been a simple and common controller of all the control techniques. In [7] position states are more penalised than the angle states. And the cart position is more penalised than angle. Here a superior performance is achieved for LQR compared two loop PID system. In [8] both swinging and stabilisation of inverted pendulum are done.

For many control applications PID control is the building block which provides optimal performance of the system. Several methods of tuning a PID are available. In [11] several tuning methods for PID are presented. In [9] PID tuning is done by pole placement technique. In [10] a tutorial is presented in which a pole placement technique with and without state estimation is introduced.

Stability is an important requirement for a control system. A good controller must stabilize a system within a specified time. In [12] pole placement in LMI regions are discussed and required conditions for stability are given. In [13] two types of regions which constitute largest class of S till date. The results when this criterion is presented in both open and close regions are used in designing methodology for control systems.

1.3 Motivation

It is practically impossible to stabilize a pendulum when in inverted position and no external force is applied. Even though the inverted pendulum seems simple from the construction point of view with force on the cart as input and cart position and pendulum angle as output, the controller design for this system is quite challenging owing to the following problems.

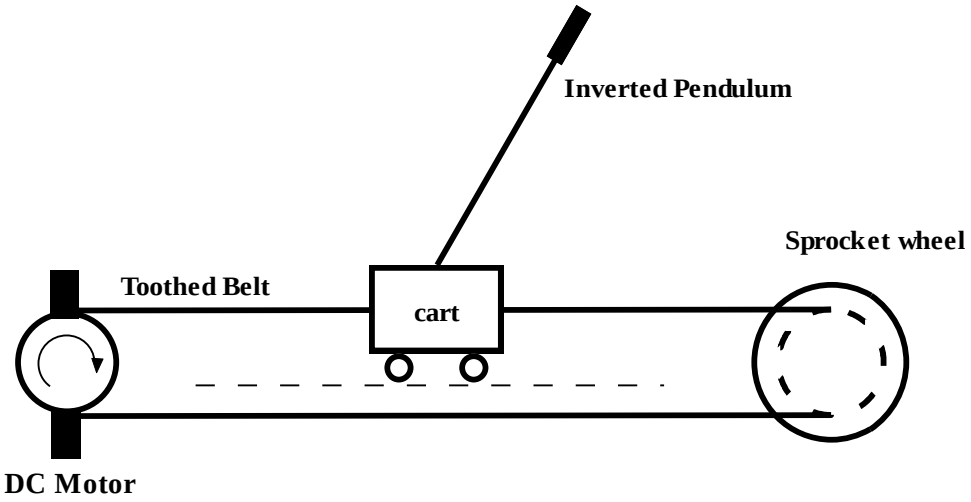

Fig 1.2 Schematic diagram of IP

1. It is a non-linear because of the presence of friction on the cart and the gravitational pull action on the pendulum.
2. It is inherently unstable
3. From the system dynamics it can be observed that the system have right hand pole zeroes which makes it a non-minimum phase system.
4. It has two degree of freedom which are cart moment and pendulum swing but only one actuator which makes the system under actuated.
5. Additionally there are constraints on control input and track length.

Due to the above challenges inverted pendulum serves as a good test bed for testing various controllers.

1.4 Objective

The aim of the project is to stabilize the inverted pendulum so that the cart position is quickly controlled and pendulum remains erect.

1. To model an inverted pendulum considering all the forces acting on it.
2. To develop various control schemes like LQR, multi loop PID and Regional pole placement technique.
3. To validate the above compensated schemes on real time model.
4. To compare the robustness of the above compensating techniques.

1.5 Organisation of the Thesis

Chapter 1 this chapter includes brief introduction on Inverted Pendulum and aits applications.

Chapter 2 This chapter includes Modelling of Inverted Pendulum and its experimental setup

Chapter 3 this chapter includes LQR control design for stabilization of Inverted Pendulum along with Simulation.

Chapter 4 this chapter includes two-loop PID controller design for Inverted Pendulum along with Simulation and Experimental results.

Chapter 5 this chapter includes Regional Pole Placement design for Inverted Pendulum along with Simulation and Experimental results.

Chapter 6 this chapter includes comparison between all designed controllers, conclusion and suggested future work

CHAPTER 2

2. MODELLING AND EXPERIMENTAL SETUP OF CART INVERTED PENDULUM

The dynamics of inverted pendulum can be derived from Newton's laws of motion. The system contains two dynamic equation one related to the cart position and the other for the pendulum angle.

2.1 Modelling of Inverted Pendulum

The parametric representation of the Inverted Pendulum system is shown in the below diagram. Let x be the distance in metres from the Y-axis, and θ be the angle in rad w.r.t vertical.

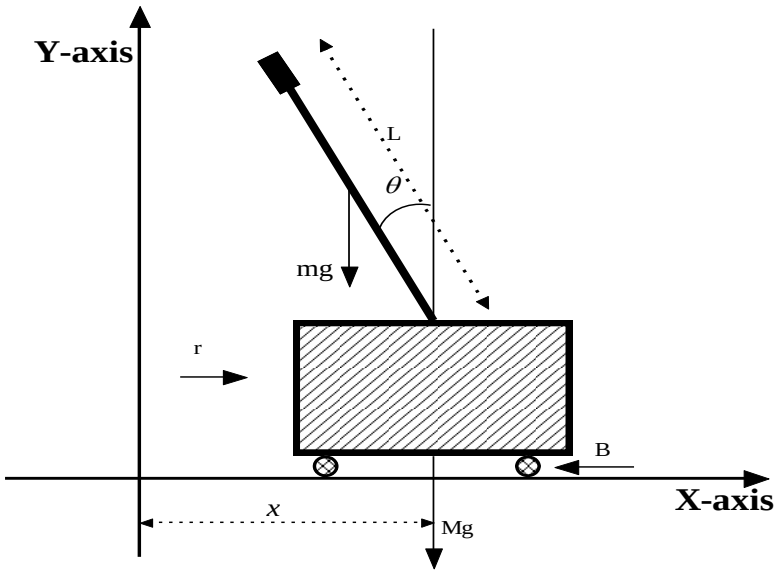

Fig2.1: *Inverted Pendulum System*

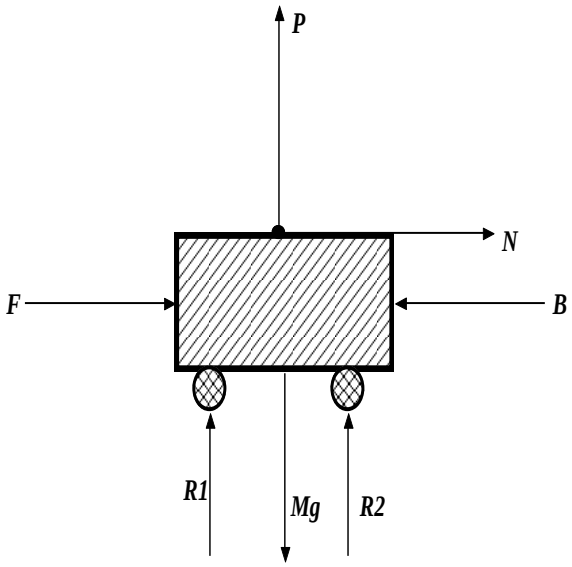

Fig 2.2: *Cart's Free Body Diagram*

From analysing the free body diagram of the cart as in Fig.2.2 we can get following conclusions,

First only horizontal forces acting on the system are considered. From this we can get the dynamics f the cart as its moment is only along horizontal axis.

.

$$Ma_X = F + N - B \tag{2.1}$$

Where a_X is taken as the acceleration in the horizontal direction.

The reaction *N* obtained is shown below in (2.2)

$$\text{N}=m\frac{d^2}{dt^2}(x + L\sin\theta) = m\ddot{x} + m\ddot{\theta}L\cos\theta - m(\dot{\theta})^2 L\sin\theta \tag{2.2}$$

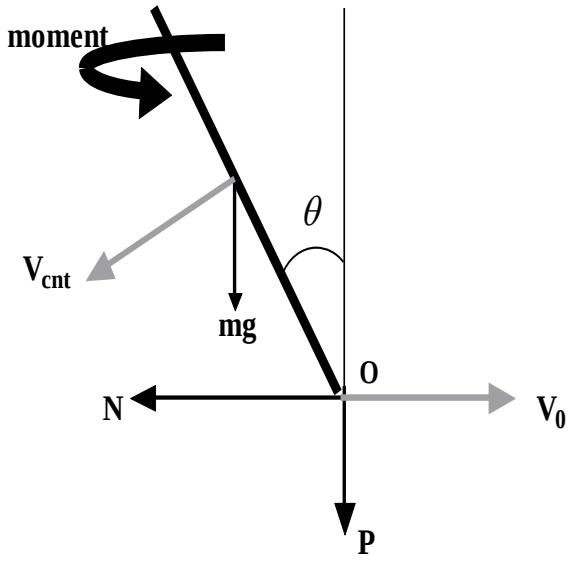

Fig.2.3: Pendulum's Free Body Diagram

Now let us consider the forces in vertical plane. The vertical reaction P given by

$$P + mg = m\frac{d^2}{dt^2}(L\cos\theta) \tag{2.3}$$

$$\text{P=mL}\ddot{\theta}\sin\theta + mL(\dot{\theta})^2\cos\theta - mg \tag{2.4}$$

The moment due to the reaction forces *P* and *N* are resolved into X and Y directions. V_{cnt} is taken as the velocity of centre of mass , V_0 is taken as the velocity of point O in the X direction. After summing all the moments across the centre we will get

$$mL\ddot{x}\cos\theta - (mL^2 + J)\ddot{\theta} = -mgL\sin\theta \tag{2.5}$$

By substituting (2.2) in (2.1) we get

$$\ddot{\theta} = \frac{mL}{\sigma}[(\text{F-b}x)\cos\theta - m(\dot{\theta})^2 L\cos\theta\,\text{sın}\,\theta + (m+M)g\,\text{sın}\,\theta] \tag{2.6}$$

By solving (2.5) and (2.6) for $\ddot{x}$ we get after simplification

$$\ddot{x} = \frac{1}{\sigma}[(\text{J+m}L^2)(F - b\dot{x} - mL\dot{\theta}^2 \sin\theta) + mL^2 g \sin\theta) + mL^2 g \sin\theta \cos\theta] \quad (2.7)$$

The parameter σ in the above equations is given by

$$\sigma = \text{m}L^2(M + m\cos\theta^2) + J(M + m) \quad (2.8)$$

Equations (2.6) and (2.7) give the dynamic equations of the cart-pendulum system dynamics.

2.2 Linearization of Inverted Pendulum model

Inverted pendulum is linearized around the equilibrium point

$$\theta = 0$$
$$\sin\theta = 0$$
$$\cos\theta = 1 \quad (2.9)$$

Linearizing (2.6) to (2.8) using (2.9)

$$\ddot{\theta} = \frac{mL}{\acute{\sigma}}[(\text{F-b}\dot{x}) + (m + M)g\theta] \quad (2.10)$$

$$\ddot{x} = \frac{1}{\acute{\sigma}}[(\text{J+m}L^2)(F - b\dot{x}) + mL^2 g\theta \quad (2.11)$$

Here $\sigma' = MmL^2 + J(M + m)$

In order to obtain the state model we consider four states cart position x, cart velocity$\dot{x}$, pendulum angle θ and pendulum angular velocity$\dot{\theta}$.

The state space will now be of the form

$$\dot{x} = Ax + Bu \quad (2.12)$$

The state space for the Inverted Pendulum system is thus given by

$$\begin{bmatrix} \dot{x} \\ \ddot{x} \\ \dot{\theta} \\ \ddot{\theta} \end{bmatrix} = \begin{bmatrix} 0 & 1 & 0 & 0 \\ 0 & \frac{-(J+mL^2)b}{\acute{\sigma}} & \frac{m^2L^2g}{\acute{\sigma}} & 0 \\ 0 & 0 & 0 & 1 \\ 0 & \frac{-(mLb)}{\acute{\sigma}} & \frac{mgL(M+m)}{\acute{\sigma}} & 0 \end{bmatrix} \begin{bmatrix} x \\ \dot{x} \\ \theta \\ \dot{\theta} \end{bmatrix} + \begin{bmatrix} 0 \\ \frac{(J+mL^2}{\acute{\sigma}} \\ 0 \\ \frac{mL}{\acute{\sigma}} \end{bmatrix} \text{F} \quad (2.13)$$

$$y = \begin{bmatrix} 1 & 0 & 0 & 0 \\ 0 & 0 & 1 & 0 \end{bmatrix} \begin{bmatrix} x \\ \dot{x} \\ \theta \\ \dot{\theta} \end{bmatrix} \tag{2.14}$$

If cart friction is neglected then we obtained a more simplified transfer function given by

$$\frac{X(S)}{F(S)} = \frac{K_{actuator}\{(J+mL^2)s^2 - mgL\}}{s^2((J(m+M)+MmL^2)s^2 - mgL(M+m))} \tag{2.15}$$

$$\frac{\theta(S)}{F(S)} = \frac{K_{actuator}(mLS^2)}{S^2((MmL^2 + (M+m)J)s^2 - MgL(M+m)} \tag{2.16}$$

Now if the values from the Feedback Digital Pendulum manual is substituted in (2.15) and (2.16) the following state space and transfer functions are obtained

Parameter	**Value**
Mass of Cart, M	2.4 kg
Mass of pendulum	.23kg
Moment of inertia, J	0.099kg-m^2
Length of Pendulum, L	0.4m
Cart friction coefficient ,b	0.05Ns/m
Acceleration due to gravity	9.81m/s^2
Actuator gain ,$K_{actuator}$	15

Table 2.1 System Parameters

$$\begin{bmatrix} \dot{x} \\ \ddot{x} \\ \dot{\theta} \\ \ddot{\theta} \end{bmatrix} = \begin{bmatrix} 0 & 1 & 0 & 0 \\ 0 & 0 & 0.238 & 0 \\ 0 & 0 & 0 & 1 \\ 0 & 0 & 6.807 & 0 \end{bmatrix} \begin{bmatrix} x \\ \dot{x} \\ \theta \\ \dot{\theta} \end{bmatrix} + \begin{bmatrix} 0 \\ 5.841 \\ 0 \\ 3.957 \end{bmatrix} u \tag{2.17}$$

$$\frac{X(S)}{F(S)} = \frac{5.841(S^2 - 6.8068)}{S^2(S^2 - 6.807)} \approx \frac{5.841}{S^2} \tag{2.18}$$

$$\frac{\theta(S)}{F(S)} = \frac{3.957S^2}{S^2(S^2-6.807)} \approx \frac{3.957}{(S^2-6.807)} \quad (2.19)$$

2.3 Experimental Setup

The setup consists of the following are the requirements [2]

- PC with PCI-1711 card
- Feedback SCSI Cable Adaptor
- Digital Pendulum Controller
- DC Motor (Actuator)
- Cart
- Pendant Pendulum with weight
- Optical encoders with HCTL2016 ICs
- Track of 1m length with limit switches.
- Adjustable feet with belt tension adjustment.
- Software: MATLAB, SIMULINK, Real-Time Workshop, ADVANTECH PCI-1711 Device driver, Feedback Pendulum Software.
- Connection cables and wires.

The two main components of the experimental set up include the cart and the pendulum. The cart moves on the track and the pendulum is fixed to it. As per the definition of the Inverted Pendulum it has to shift its centre of gravity above its reference point which leads to instability. The DC servo motor drives the cart and the force with which it drives the cart is proportional to the control voltage applied.

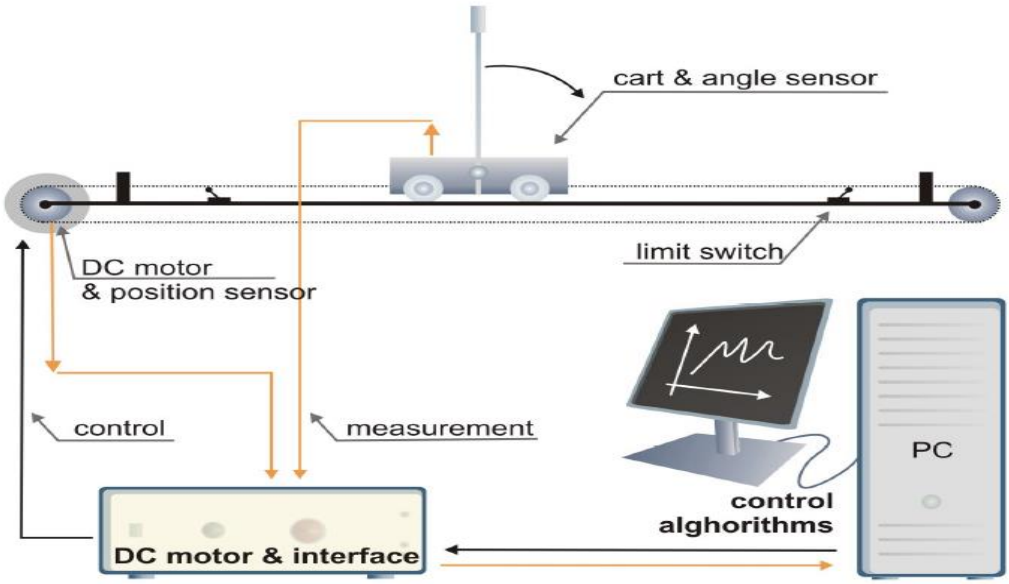

Fig.2.4: .Feedback's Digital Pendulum Experimental Setup Schematic [3]

The cart's moment on the track is limited for the safety. It is done by using two limit switches which will shut down the power to the cart when activated. The cut way diagram in the fig 1.7 shows the location of sensors and switches on the track. There are digital encoders mounted on the track which outputs a signal that is a combination of two signals 90^0 apart one representing shaft position and the other direction of rotation. Two such digital encoders are used one for the cart and the other for the pendulum. Fig 1.9 shows the operating principle of optical encoder.

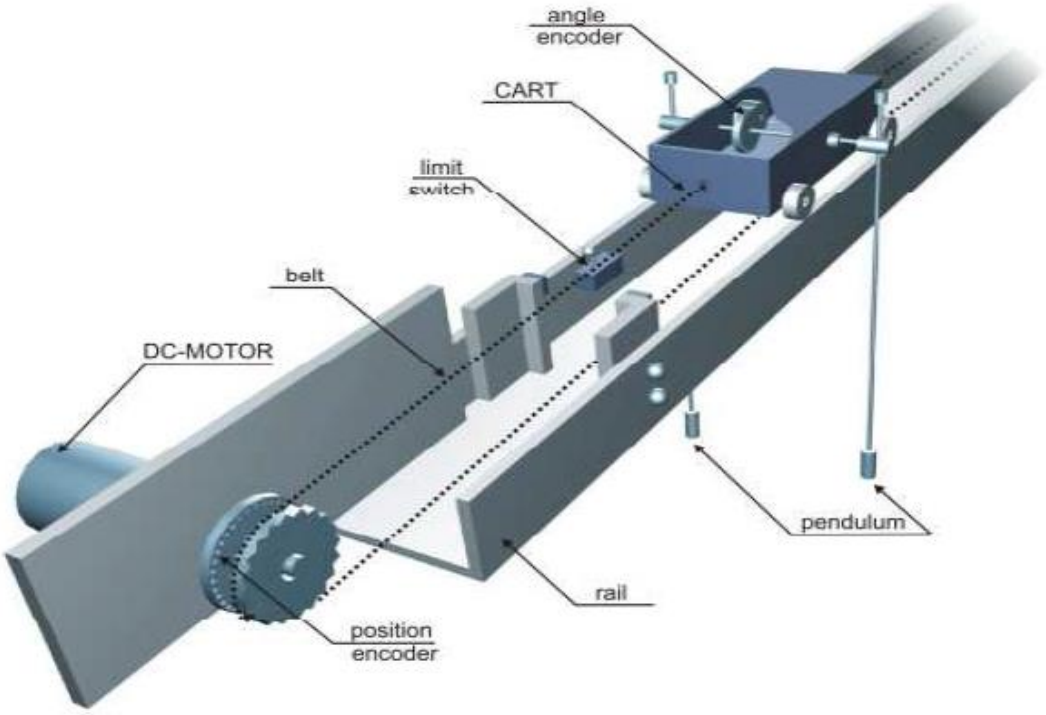

Fig.2.5: Cutaway Diagram Showing sensors and their mounting [2]

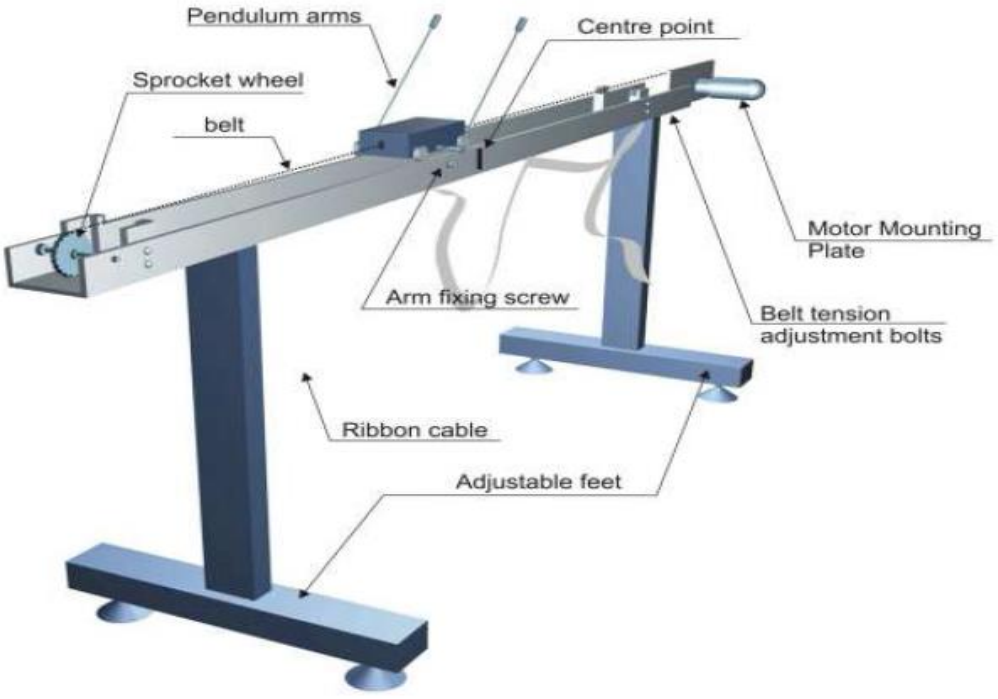

Fig.2.6 .Digital Pendulum Mechanical Setup [2]

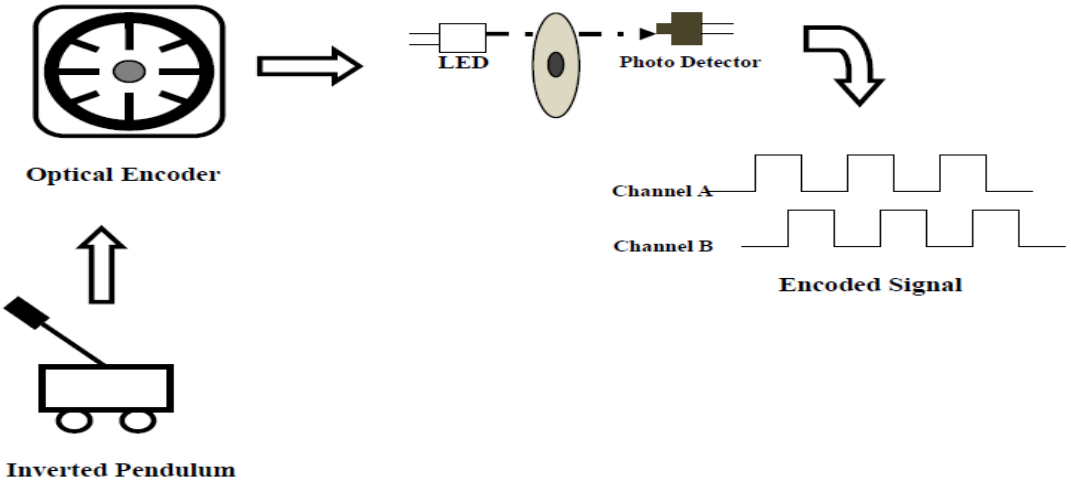

Fig.2.7: Optical Encoder operating principle

.

The implementation of controller in real time is done by designing a specific controller in MATLAB Simulink and then applying it on the real time model. The fig 1.10 shows the algorithm for working of this Inverted Pendulum Real Time Workshop.

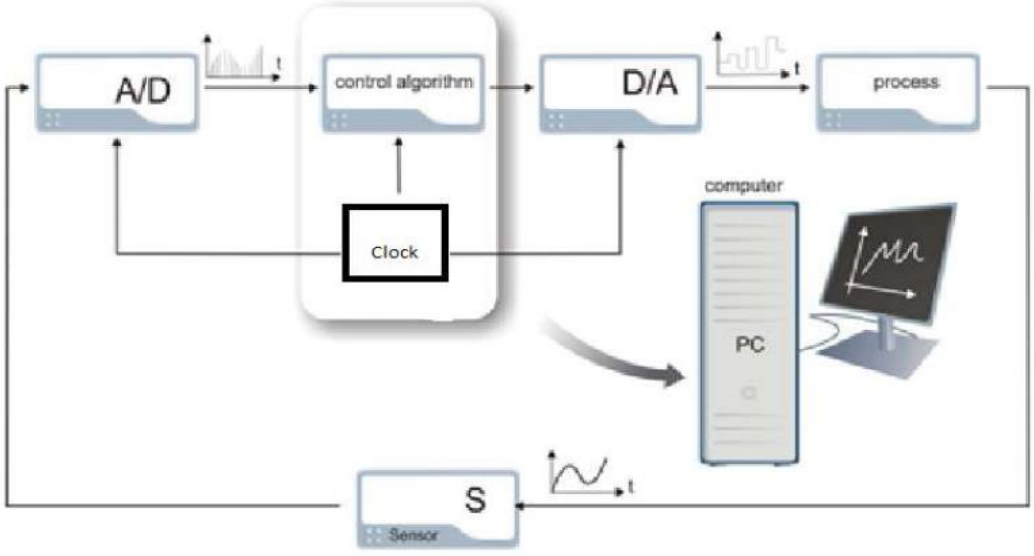

Fig.2.8: Computer based Control Algorithm [2]

The working of A/D, D/A and control algorithm depends on the clock pulses supplied by the clock.

2.4 Real-Time Workshop

Continuous programming applications [5]. It has the accompanying highlights

- Automatic code era customized for different target stages.
- A fast and direct way from framework configuration to execution.
- Seamless mix with MATLAB and SIMULINK.
- A straightforward graphical client interface.
- An open building design and extensible make process.

The tool stash has a programmed project building procedure for ongoing procedures. Fig.1.11 clarifies the procedure diagrammatically. An abnormal state m-record controls this fabricate process.

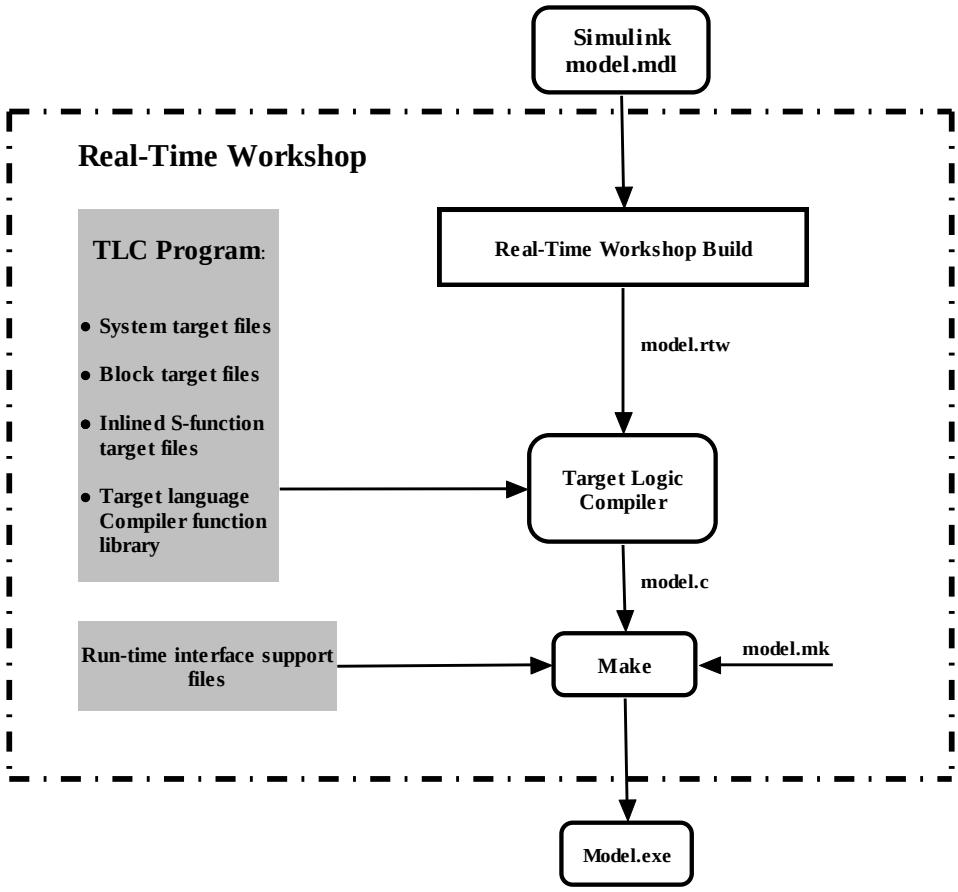

Fig.2.9: .Real-Time Workshop working schematic [5]

For a real time build process following steps are involved [5]

1. Ongoing Workshop examinations the square chart and orders it into a middle of the road various levelled representation of the structure model.rtw.
2. The Objective Dialect Compiler (TLC) peruses the model.rtw and proselytes it into C code that is set in the fabricate catalog inside of the MATLAB working index.
3. The TLC develops a makefile from a suitable target makefile layout and spots in the fabricate registry.
4. The framework make utility peruses the makefile to assemble the source code and connections article documents and libraries and create an executable document model.exe.

This basic executable record is effortlessly seen by equipment as it is in double. Consequently the control calculation in abnormal state dialect is consistently changed over into an executable program by the tool kit. The following segment presents the handy issues that need to be tended to while outlining any controller to Inverted Pendulum frameworks**.**

CHAPTER 3

3. LINEAR QUADRATIC REGULATOR (LQR) DESIGN TO STABILIZE INVERTED PENDULUM

In LQR according to the desired characteristics weight matrix is chosen by iterative process, depending on the weight provided for the cost function by solving Recatti equation optimal control is obtained. The part presents a brief portrayal of the LQR idea. The focuses to be remembered before planning a LQR based state criticism are additionally given. Since, the decision of the LQR is the key towards LQR outline, a methodical weight choice for the CIPS is introduced..

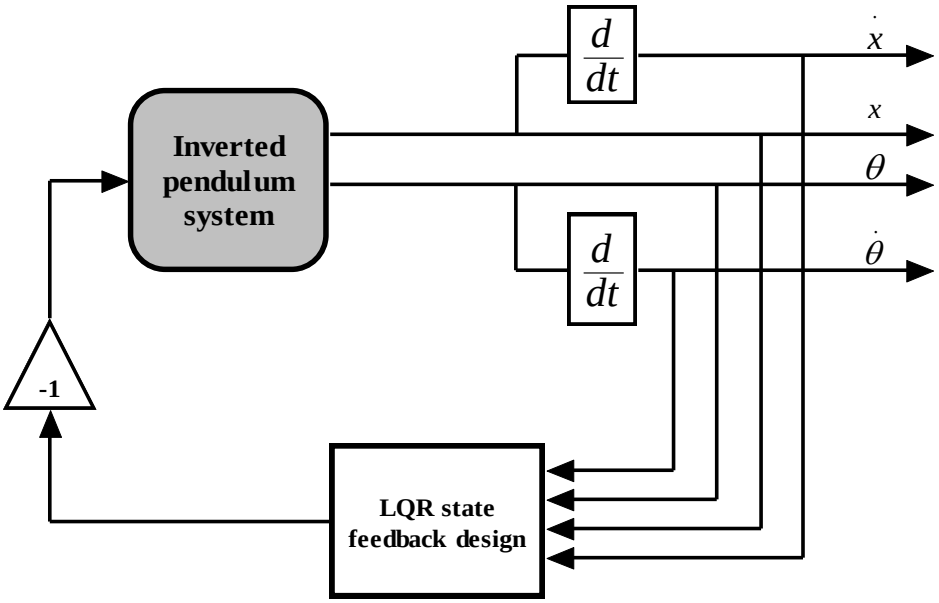

Fig: 3.1 Block diagram for LQR on IP

3.1 Introduction

The LQR is a standout amongst the most broadly utilized static state feedback methods, basically as the LQR based pole placement helps us to make an interpretation of the performance constrints into different weights in the execution record. This flexibility is the sole explanation behind its notoriety. As seen in Chapter 1 the inverted pendulum framework has numerous physical constraints both in the states and in the control. Consequently, the LQR

outline is endeavoured. The decision of the performance indices relies upon physical requirements and performance of the system. State feedback of any system can be summed up for a LTI framework as given beneath:

$$\dot{x} = Ab + Bu$$
$$Y=Cx \tag{3.1}$$

In the event that all the n states are accessible for input and the states are totally controllable then there exists a FB gain matrix K, such that the control input would be

$$u = -K(x - x_d) \tag{3.2}$$

Now taking x_d as the desired state vector we get the closed loop dynamic equations from (3.1) and (3.2) given by

$$\dot{x} = (A - BK)\, x + BKx_d \tag{3.3}$$

Decision of K relies on upon the pole locations required, where one means to place the poles in a way that performance is achieved as per our requirement. On account of LQR the control is subjected to a Cost Functional (CF) or Performance Index (PI) which is given as

$$J=\frac{1}{2}[(z(t_f) - y(t_f)]^T F(t_f)\big[z(t_f) - y(t_f)\big] + \frac{1}{2}\int_{t_0}^{t_f}\{[[z - y]^T Q[z - y] + u^T Ru\}dt \tag{3.4}$$

Q--- Error Weighted Matrix
R--- Control Weighted Matrix
F--- Terminal Cost Weighted Matrix

Let z be the reference vector of m^{th} dimension and u be the input vector of r^{th} dimension. On the off chance that all the states are accessible in the yield for input then m gets to be n. Since, the PI (3.4) is seen to be having error and control in quadratic terms it can be termed as quadratic CF. In the event that our goal is to keep the state to close to zero then it is called as a state regulatory system

- Each and every weighted matrix is symmetric.

- To keep the squared error positive the matrix Q (error weighted matrix) is taken to be positive semi-definite. In general Q is taken to be a diagonal matrix.
- In order to keep the control always positive R matrix is chosen to be semi definite one
- TO make sure that the error e(t) to take a small value within a finite time of t_f F matrix is to be taken as positive semi-definite matrix all the time.

The CF will now be

$$J = \int_{t_0}^{\infty} \frac{1}{2}\{\acute{x}Qx + \acute{u}Ru\}dt \tag{3.5}$$

If we apply Pontryagin's Maximum Principle for an OL system we get an optimal solution for the CL system resulting in the equations given below

$$\begin{gathered} \dot{x} = Ax + Bu, x(t_0), x(t_0) = x_0 \\ \dot{\lambda} = -Qx - \dot{A}^T\lambda, \lambda(t_f) = 0 \\ Ru + B^T\lambda = 0 \end{gathered} \tag{3.6}$$

From the nature of the equation (3.6) which is linear and inn order to connect these equations we use the following relation

$$\begin{gathered} \lambda = Px \\ \dot{\lambda} = P\dot{x} + \dot{P}x \end{gathered} \tag{3.7}$$

Substituting the value of $\dot{x}, \dot{\lambda}$ from equation (3.6) in equation (3.7) and then substituting the value of u from (3.6) the following equation is obtained

$$PAx + A^TPx + Qx - PBR^{-1}Px + \dot{P}x = 0 \tag{3.8}$$

Thus the obtained equation is Matrix Ricatti Equation and solution is given by

$$PA + A^TP + Q - PBR^{-1}P = 0 \tag{3.9}$$

The control input fo the above Algebraic Riccati Equation (ARE) is obtained from

$$Ru + B^T\lambda = 0 \text{ as}$$
$$u = -R^{-1}B^TPx$$
$$u = -Kx \tag{3.10}$$

3.2. LQR Control Design

The decision of Q and R is imperative as the entire LQR state input arrangement relies on upon their decision. Typically they are picked as identity values and are progressively iterated to get the controller parameter. The value of R is chosen to be a scalar value since it is a single input system.

The excitation because of initial condition observed in the states can be dealt with as an undesirable deviation. On the off chance that the system depicted is controllable then it can be drive the system to its required equilibrium point. In many cases, it is extremely hard to keep the control input inside of bound as chances are such that the control sign would be high which will make the actuator to get saturated and would oblige high bandwidth models. Thus, it is needed to have an exchange off between the requirement for regulation and the extent of the control signal. It can be seen that the decision of R comes helpful in limiting the control signal. So by choosing a larger value for R we get a smaller value of control input. It can be seen that bigger the weight on R the littler is the control signal. The rationale behind decision of weights of Q (normally picked as a slanting grid) is relative that the state that obliges more control requires more weightage than the state that obliges less control.

Algorithm:

The logic behind choosing the weights is that the states which require more control require more weight. For the weight(R) on the control signal it is such that larger the value of R smaller is the control signal.

- Choose$Q = diag(q1, q2, q3, q4)$ as the weight matrix, where q_1 term corresponds to the weight on cart position, q_2 corresponds to the weight on cart linear velocity, q_3 corresponds to the pendulum angle, and q_4 corresponds to the angular velocity
- Since the cart position is to be at zero and that constraint is difficult to obtain we add more weight to the cart position .thus we choose $q_1 \gg q_{2,}q_3, q_4$

- In order to make up for the falling pendulum the velocity of cart should change rapidly compared to the pendulum angular velocity, so $q_2 \gg q_4$.
- Due to the physical constraints imposed on the pendulum angle and cart position we We choose $q_1 \gg q_2, q_{3\gg} q_4$ due to constraints on cart position and pendulum angle.

By iterative process the value of gains obtained are K_1 = -2.2361 K_2 = -3.1803 K_3 = 73.8623 K_4 =29.219

3.3 Results and Discussion

SIMULATION RESULTS

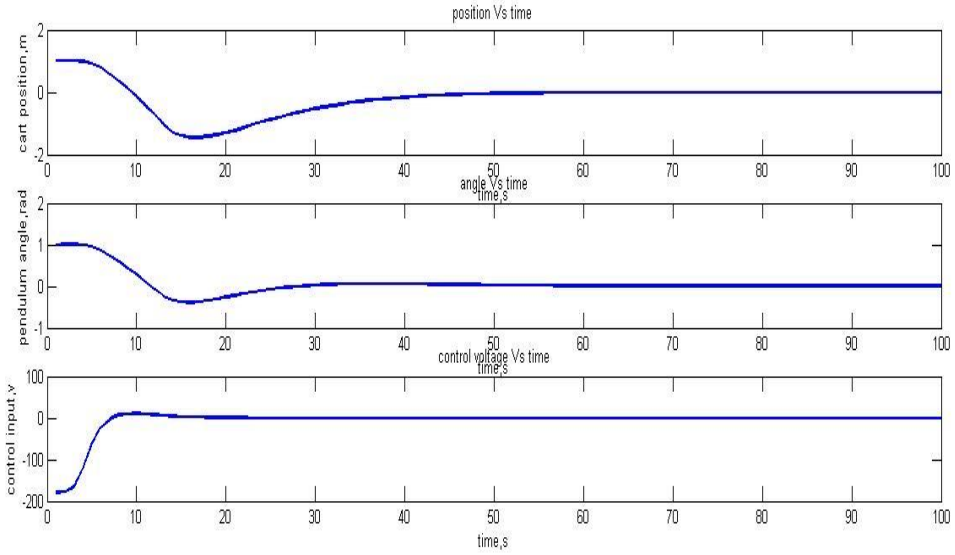

FIG: 3.2 simulation result for LQR on IP

3.4 Chapter Summary

The Chapter starts with the explanation of LQR how it implemented and its design methodology. . Different focuses that need to be considered in the outline of LQR are additionally given. Accordingly, the section exhibits a calculation for choice of LQR weights. Accordingly, the section exhibits a calculation for choice of LQR weights. The chapter is concluded with the simulation result.

CHAPTER 4

4. TWO-LOOP PID CONTROLLER DESIGN FOR INVERTED PENDULUM

For many control problems, PID control module is the building block which provides the regulation and disturbance rejection for single loop, cascade loop, multi loop and multi input and multi output control schemes. Over decades PID control technology has undergone many changes and today the controller may be standard utility routine with in supervisory system software, a dedicated hardware process control unit which can be used for control system construction. Several methods exist to tune a PID controller but in this design we use pole placement method.

4.1 Introduction

The fig 4.1 shows the block diagram of a PID controller. The controller output depends on the error signal generated. The control signal u can be mathematically represented by [14]

$$e = r - y$$

$$u = K_P e + K_I \int e\, dt + K_D \frac{de}{dt} \tag{4.1}$$

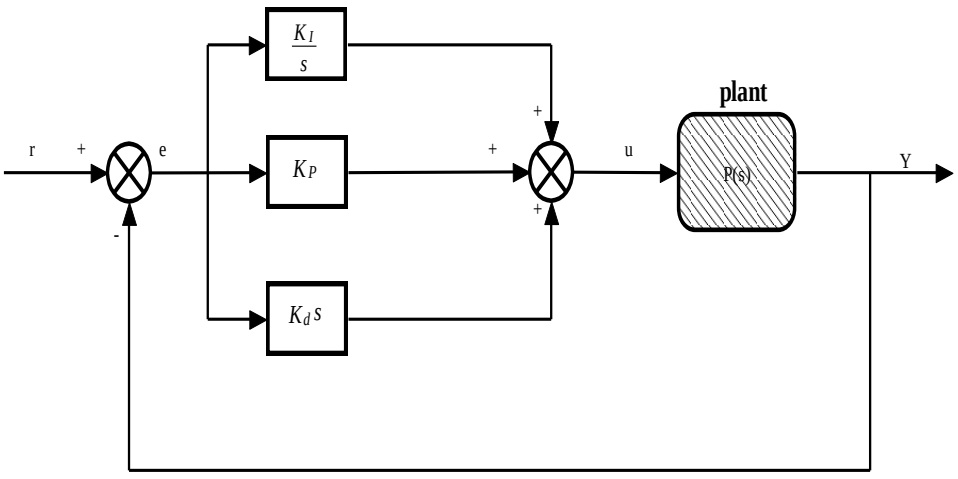

Fig 4.1: PID Controller for a Closed Loop System

It is observed that the error get enormously decreased by increasing the value of K_P yet the reaction turns out to be exceedingly oscillatory. At the same time, a consistent steady state error persists. The integral controller term K_I guarantees that the error goes to zero. Anyway if the value of K_I is increased it leads to a sluggish response. The derivative control term K_D makes sure that the system response settles quickly by damping the oscillatory part. Utilization of high estimation of K_D ma lead to instability. In this way, so as to accomplish acceptable execution we have to pick these qualities carefully. There exist numerous blocking tuning methods of which Ziegler-Nichols tuning is a well-known one.

At first, the on-off controller was generally utilized. Yet, because of high oscillatory nature of output the on-off offered path to the proportional controller. The control activity on account of P sort criticism will be specifically relative to the slip produced. By using this Proportional controller the control output form the controller is directly proportional to the error signal generated. Decision of K_P is a compromise between these two clashing necessities. It might be noticed that the issue of high gain causes instability while in closed loop. Integral action being a necessary activity has been an important abhorrence in control loops. It has the benefit of ensuring a zero error, however at the expense of decrease in the speed. On the other hand addition of derivative controller improves the speed of the response.

4.2 Controller Design

Control structure for PID is as shown in figure: 4.2. As in [15] two PID controllers are used C1, C2. Reference values for cart position and pendulum angle are taken as 0.

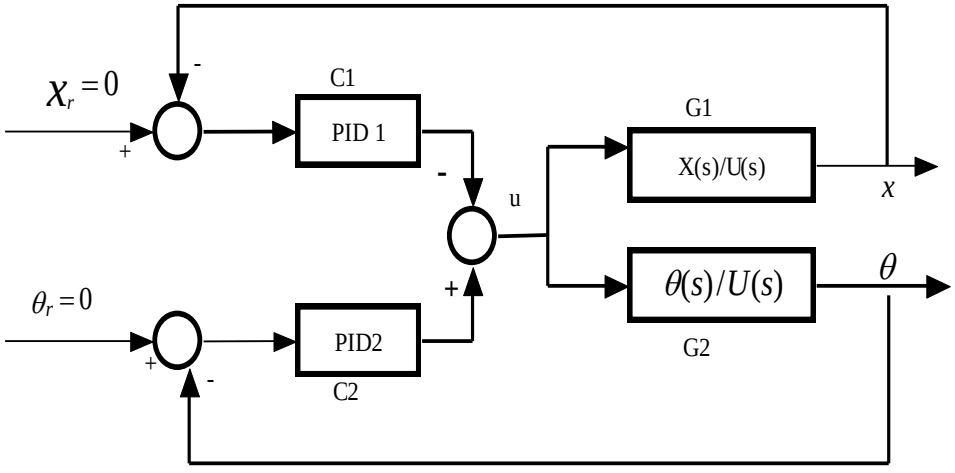

Fig: 4.2 block diagram for two loop PID controller

The characteristic equation for the controller in fig 4.2 will be

$$1 - G_1C_1 + G_2C_2 \tag{4.2}$$

Where C1 and C2 are two PID Controllers. G_1 and G_2 are represented by plant transfer functions where b1=0.3894, b2=0.2638 and a²=6.807.

$$1 - \frac{b_1}{s^2}\frac{\left(K_{d_1}s^2 + K_{p_1}s + K_{i_1}\right)}{s} + \frac{b_2}{(s^2 - a^2)}\frac{\left(\left(K_{d_2}s^2 + K_{p_2}s + K_{i_2}\right)\right.}{s} = 0 \tag{4.3}$$

From LQR we get the desired pole locations and from these pole locations the characteristic equation formed will be

$$s^5 + 26.4s^4 + 218.6s^3 + 871.3s^2 + 1721.8s + 1343.7 = 0 \tag{4.4}$$

Now using pole placement technique the gains of PID controllers are obtained as follows

$$\begin{bmatrix} -b_1 & 0 & 0 & -b_2 & 0 & 0 \\ 0 & -b_1 & 0 & 0 & -b_2 & 0 \\ a^2b_1 & 0 & -b_1 & 0 & 0 & -b_2 \\ 0 & a^2b_1 & 0 & 0 & 0 & 0 \\ 0 & 0 & a^2b_1 & 0 & 0 & 0 \end{bmatrix} \begin{bmatrix} Kd_1 \\ Kp_1 \\ Ki_1 \\ Kd_2 \\ Kp_2 \\ Ki_2 \end{bmatrix} = \begin{bmatrix} p_1 \\ p_2 + a^2 \\ p_3 \\ p_4 \\ p_5 \end{bmatrix} \tag{4.5}$$

After substitution we get:

$$\begin{bmatrix} -5.841 & 0 & 0 & -3.957 & 0 & 0 \\ 0 & -5.841 & 0 & 0 & -3.957 & 0 \\ 39.759 & 0 & -5.841 & 0 & 0 & -3.957 \\ 0 & 39.759 & 0 & 0 & 0 & 0 \\ 0 & 0 & 39.759 & 0 & 0 & 0 \end{bmatrix} \begin{bmatrix} Kd_1 \\ Kp_1 \\ Ki_1 \\ Kd_2 \\ Kp_2 \\ Ki_2 \end{bmatrix} = \begin{bmatrix} 26.4 \\ 225.07 \\ 871.3 \\ 1721.8 \\ 1343.7 \end{bmatrix} \tag{4.6}$$

For $\mathbf{C_1}$: –

$$Kp_1 = 43.3, Ki_1 = 33.796, Kd_1 = 2.254 \tag{4.7}$$

For $\mathbf{C_2}$: –

$$Kp_2 = 120.9, Ki_2 = 247.43, Kd_2 = 10 \quad (4.8)$$

The obtained controller design is applied on the real time model. Here a second velocity filter with the transfer function as shown in (4.9) after the derivative block in PID controller. This filters out noise to some extent.

$$F(s) = \frac{10000}{s^2 + 70.7s + 10000} \quad (4.9)$$

4.3 Results and Discussion

SIMULATION RESULT

The figure 4.3 shows the simulation result for two loop PID controller on Inverted Pendulum model.

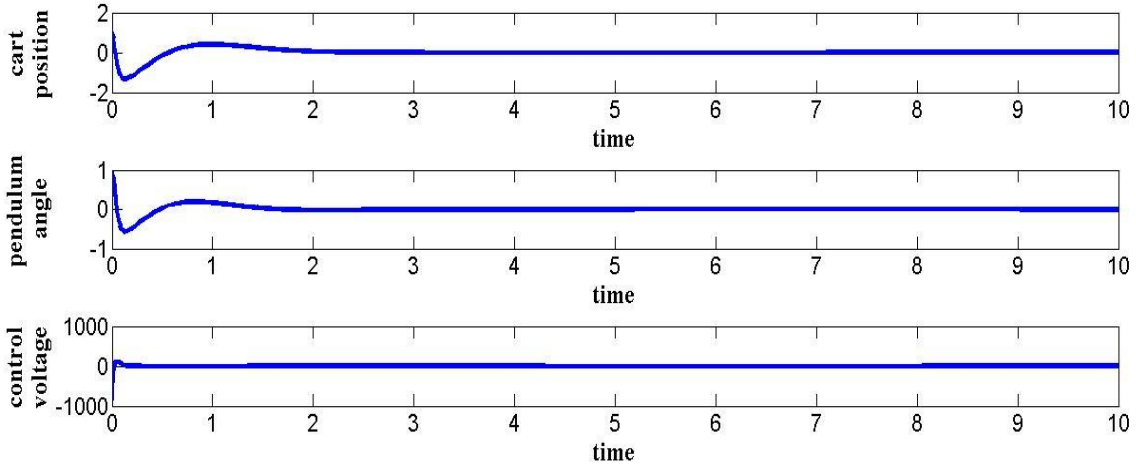

Fig: 4.3 Two-loop PID controller simulation result.

EXPERIMENTAL RESULTS

On the application of controller design on the real time model the following result is obtained. It can be seen that the oscillations on the cart position sustain, this is due too the unfiltered noise which is not being filtered.

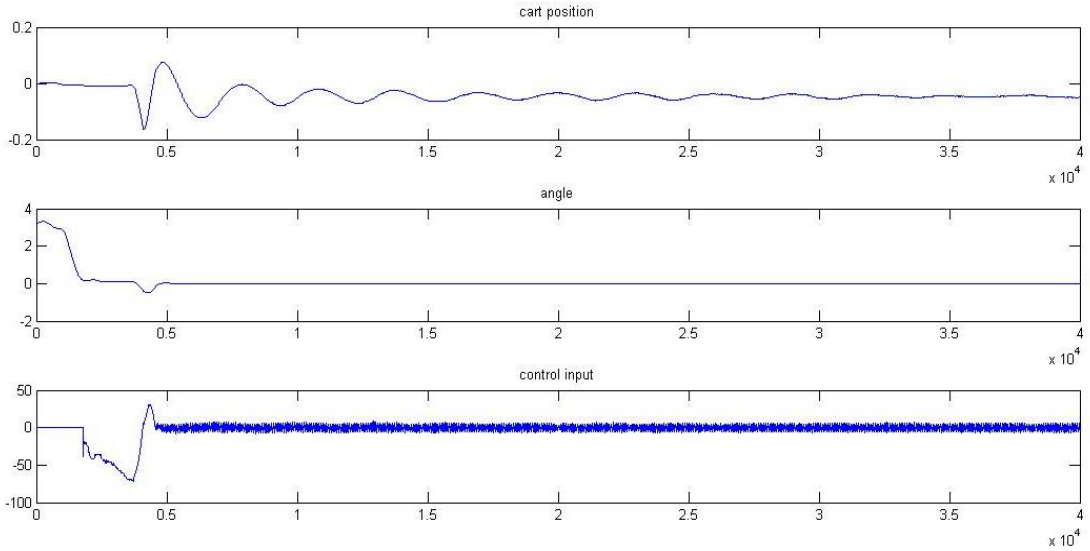

Fig4.4: Experimental result for two-loop PID controller

Increase in gain:

Fig: is obtained by increasing the gain. It can be noted that the system get marginally stable when gain is 5 after that point the cart position exceeds 0.3m after which the system becomes unstable

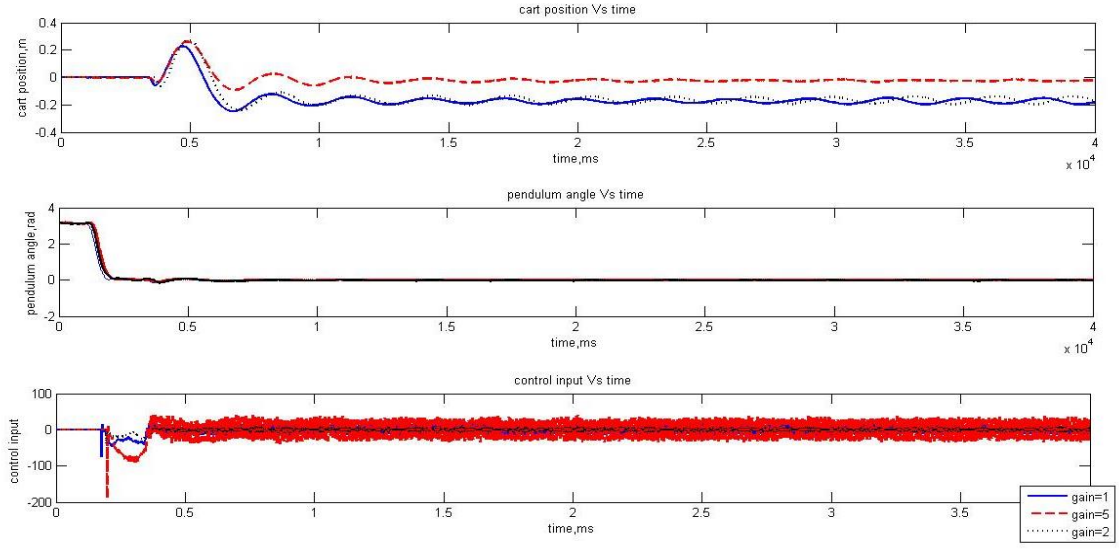

Fig 4.5: Experimental result for two-loop PID controller when gain is increased

Decrease in gain:

Fig: is obtained by decreasing the gain. It can be noted that the system get marginally stable when gain is reduced to .5 after that point the cart position exceeds 0.3m after which the system becomes unstable

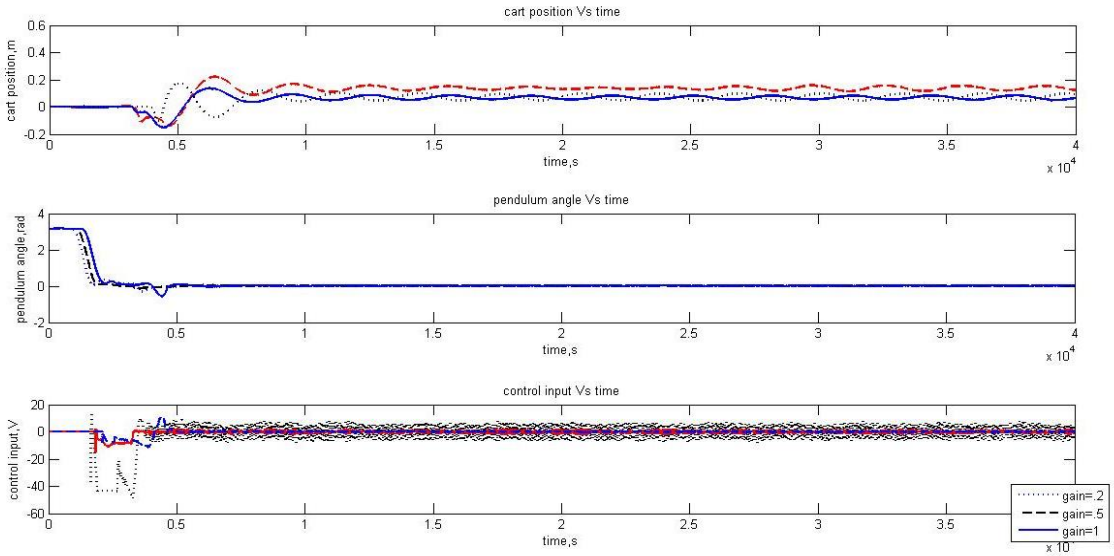

Fig 4.6: Experimental result for two-loop PID controller with decrease in gain

Delay:

A delay is introduced in the system and the results are obtained as shown in the fig: Its observed that after a delay of .05 the system goes unstable.

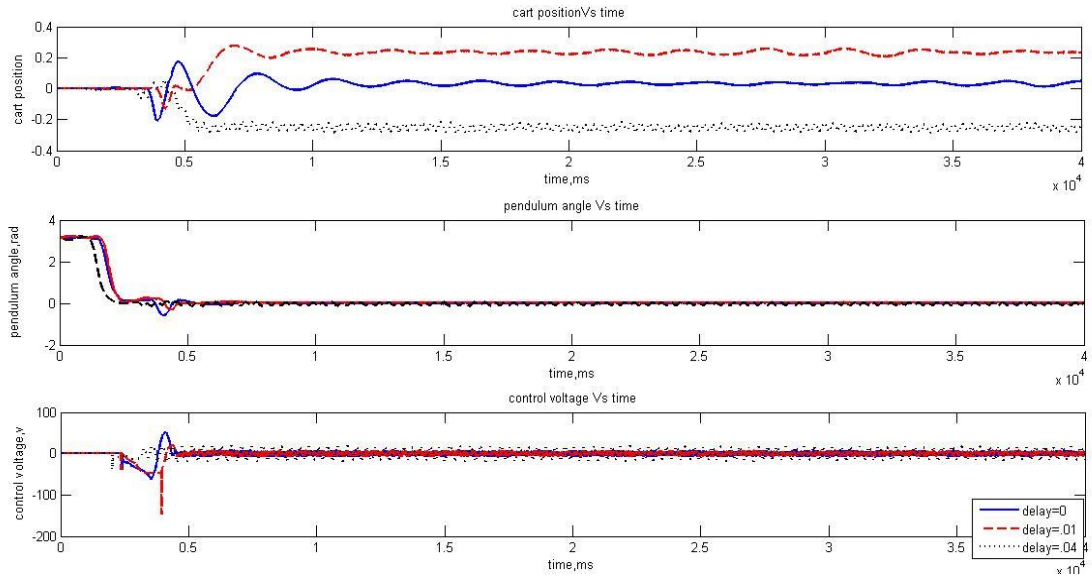

Fig 4.7: Experimental result for two-loop PID controller with delay

Two loop PID controller Robustness summary

	Gain margin	Gain cross over frequency	Phase margin
Simulation	(.2238,2.2)	27.4	.034
Experiment	(.2,5)	----	.04

Table 4.1 robustness summary

4.4 Chapter Summary

The chapter begins with the introduction to PID control and its design constraints. Here the closed loop poles obtained from LQR design are taken and by using pole placement design Two Loop PID Controller is designed. Its simulation is done in MATLAB and applied on real time workshop. From the experimental results it can be observed that WITH a two loop PID control sufficient performance is obtained.

CHAPTER 5

5. REGIONAL POLE PLACEMENT TECHNIQUE TO STABLIZE INVERTED PENDULAM

The basic necessity of any control system is stability. A good controller has to provide well-damped response sufficiently. If the position of the poles are so adjusted in complex plane such that the desired performance is achieved then such a technique is called Regional Pole Placement. Contrary to the traditional pole placement techniques here a complete region is specified instead of specific points. Complex region may include regions like conic sector, disc, half plane etc.

5.1 Introduction

COMPLEX PLANE AS LMI REGION

A region in complex plane can be represented by means of LMI as in [12]. A function is specified as of LMI to describe a region and it's called as Characteristics equation of the region.

For example left half of complex plane can be described as simple function of $f: z + \bar{z} < 0$. All the points in the left of plane satisfies the condition. Similarly we can specify right half of plane by reversing the inequality. One can link the above objective to Lyapunov's stability criteria to design pole placement controller.

An LMI region is any subset $\mathcal{D}$ of the complex s-plane that can be expressed as

$$\mathcal{D} = \{z \epsilon \mathbb{C}: L + zM + \bar{z}M^T < 0\} \quad (5.1)$$

Where L and M are real matrices and $L^T = L$, and $M = M_1^T M_2$ the matrix function

$$f_{\mathcal{D}}(z) = L + zM + \bar{z}M^T$$

The equation (5.1) is the characteristic function of the complex plane $\mathcal{D}$.

LMI regions incorporate diverse areas, for example, half s-plane, circles, conics sectors, strips, and any convergence of the above. For such diverse LMI areas "Lyapunov theorem" is accessible. For entries $(\lambda_{ij})_{1 \le i,j \le m}$ and $(\mu_{ij})_{1 \le i,j \le m}$ in matrices L and M, matrix A is said to

have all its eigenvalues in a specific complex plane $\mathcal{D}$ only if there is a a positive definite matrix P which satisfy the equation (5.3)

$$\{\lambda_{ij}P + \mu_{ij}AP + \mu_{ji}PA^T\}_{1\leq i,j\leq m} < 0. \tag{5.3}$$

5.2 LMI Regions

Various LMI regions like half plane, disc, conic and their characteristic equations have been described below [12]

- For a Half-plane region, the characteristic equation is given by (5.4)

$$Re(z) < -\propto:\ f_{\mathcal{D}}(z) = z + \bar{z} + 2 \propto < 0 \tag{5.4}$$

- For a disk region centred at $(-q, 0)$ with radius r the characteristic equation is given by (5.5):

$$f_{\mathcal{D}}(z) = \begin{bmatrix} -r & q+z \\ q+\bar{z} & -r \end{bmatrix} < 0 \tag{5.5}$$

- For a conic sector region with inner angle 2θ and apex at the origin the characteristic equation is given by(5.6)

$$f_{\mathcal{D}}(z) = \begin{bmatrix} sin\theta(z+\bar{z}) & cos\theta(z-\bar{z}) \\ cos\theta(\bar{z}-z) & sin\theta(z+\bar{z}) \end{bmatrix} < 0 \tag{5.6}$$

.

- For the entire Left half-plane the characteristic equation obtained is given by equation (5.7)

$$f_{\mathcal{D}}(z) < 0 \Leftrightarrow z + z^T < 0 \tag{5.7}$$

For this section $L = 0$ and $M = 1$has to be taken and the LMI derived is given by (5.8)

$$AX + XA^T < 0 \tag{5.8}$$

- ∝ −Stability

$$f_{\mathcal{D}}(z) < -\propto \Leftrightarrow 2 \propto + z + z^T < 0 \tag{5.9}$$

For this section $L = 2 \propto$ and $M = 1$has to be taken and the LMI derived is given by (5.8)

$$2 \propto X + AX + XA^T < 0 \tag{5.10}$$

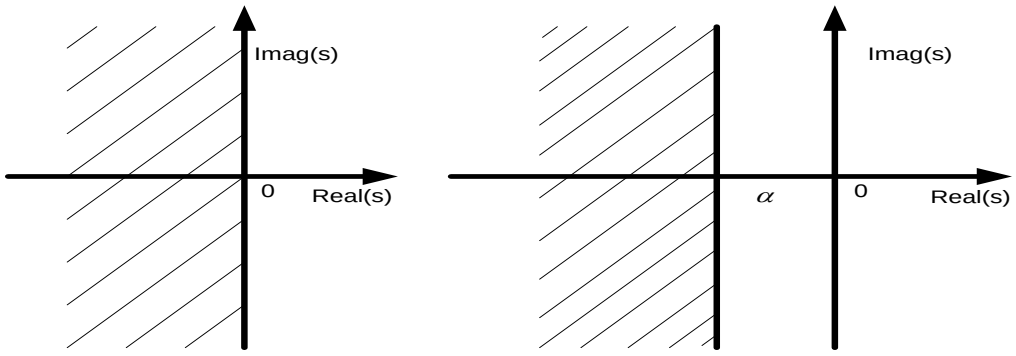

Fig: 5.1 ∝-stable LMI region

Disk

Disk of Radius r, Centred at $(q, 0)$ [24], [12]

$$|z - q| < r \;\Leftrightarrow \begin{bmatrix} -r & z-q \\ \bar{z}-q & -r \end{bmatrix} < 0 \tag{5.11}$$

It is sufficient to take the matrices:

$$L = \begin{bmatrix} -r & -q \\ -q & -r \end{bmatrix}, M = \begin{bmatrix} 0 & 1 \\ 0 & 0 \end{bmatrix} \tag{5.12}$$

This gives the following LMI for disk region:

$$\begin{bmatrix} -rX & -qX + AX \\ -qX + XA^T & -rX \end{bmatrix} < 0 \tag{5.13}$$

For example take $r = 1$ and $q = 0$ we obtain

$$A^T XA - X < 0. \tag{5.14}$$

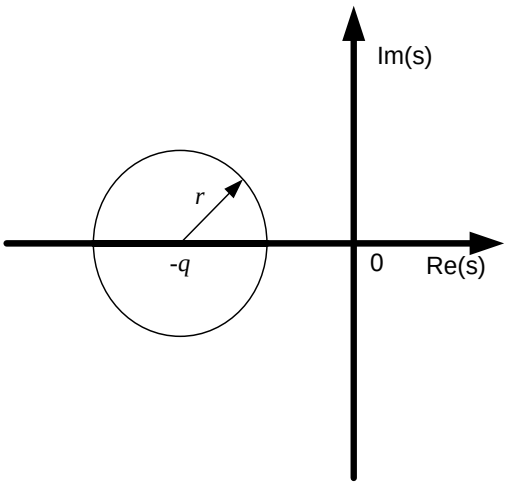

Fig 5.2 disc sector LMI region

Conical Sector

$$a.Re(z) + |b.Im(z)| < 0 \Leftrightarrow \begin{bmatrix} a(z+\bar{z}) & -b(z-\bar{z}) \\ b(z-\bar{z}) & a(z+\bar{z}) \end{bmatrix} < 0 \tag{5.15}$$

It is sufficient to take the matrices

$$L = \begin{bmatrix} 0 & 0 \\ 0 & 0 \end{bmatrix}, \qquad M = \begin{bmatrix} a & -b \\ b & a \end{bmatrix} \tag{5.16}$$

This gives the following LMI for conic sector region:

$$\begin{bmatrix} a(AX + XA^T) & -b(AX - XA^T) \\ b(AX - XA^T) & a(AX + XA^T) \end{bmatrix} < 0 \tag{5.17}$$

It's known that

$$0 < \theta < \frac{\pi}{2}, \cos(\theta) = \frac{-b}{\sqrt{a^2 + b^2}}, \sin(\theta) = \frac{a}{\sqrt{a^2 + b^2}} \tag{5.18}$$

Thus the obtained LMI region is given by (5.19)

$$\begin{bmatrix} \sin(\theta)(AX + XA^T) & \cos(\theta)(AX - XA^T) \\ -\cos(\theta)(AX - XA^T) & \sin(\theta)\,(AX + XA^T) \end{bmatrix} < 0 \tag{5.19}$$

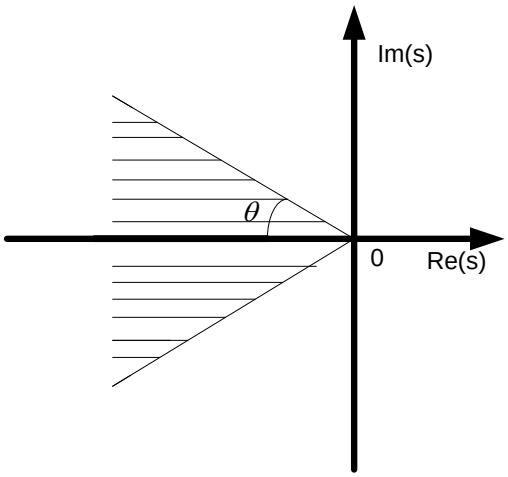

Fig 5.3 conical sector LMI region

OUTPUT FEEDBACK REGIONAL POLE PLACEMENT CONTROLLER

Consider a controller which places poles in a desired LMI region [12]

Let the state-space equation for an LTI plant be as shown in the equation (5.20)

$$\acute{P}\begin{cases} \dot{x} = Ax + B_w w + Bu \\ z = C_z x + D_{zw} w + D_z u \\ y = Cx + D_w w + D_{yu} u \end{cases} \tag{5.20}$$

The required LMI region is given by

$$\mathcal{D} = \{z \epsilon \mathbb{C} : L + zM + \bar{z}M^T < 0\} \tag{5.21}$$

Let the required controller which places the poles in desired LMI region $\mathcal{D}$ be given by

$$K\begin{cases} \dot{x}_K = A_K x_K + B_K y \\ u = C_K x_K + D_K y \end{cases} \tag{5.22}$$

The state space equation for the closed loop transfer function after the introduction of controller with control law Ky is given by

$$\begin{aligned} \dot{x}_{cl} &= Ax_{cl} + Bw \\ z &= Cx_{cl} + Dw \end{aligned} \tag{5.23}$$

Where

$$A = \begin{bmatrix} A + BD_K C & BC_K \\ B_K C & A_K \end{bmatrix} \tag{5.24}$$

$$B = \begin{bmatrix} B_w + BD_K D_w \\ B_K D_w \end{bmatrix} \tag{5.25}$$

$$C = [C_z + D_z D_K C \quad D_z C_K] \tag{5.26}$$

$$D = [D_{zw} + D_z D_K D_w]. \tag{5.27}$$

For robust $\mathcal{D}$-stability of the system there should exist a positive definite matrix X such that

$$\begin{bmatrix} \mathrm{M}_{\mathcal{D}}(\mathrm{A},\mathrm{X}) & M_1^T \otimes (XB) & M_2^T \otimes C^T \\ M_1 \otimes (B^T X) & -\gamma I & I \otimes D^T \\ M_2 \otimes C & I \otimes D & -\gamma I \end{bmatrix} < 0 \tag{5.28}$$

Where $M_1^T M_2 = M$

[13] *Theorem: O*utput feedback controller $K(s)$and a symmetric matrix $X > 0$ exist such that (21) holds if and only if two $n \times n$ positive symmetric matrices R and S and matrices A_K, B_K, C_K, D_K exists such that

$$\Lambda(R,S) = \begin{bmatrix} R & I \\ I & S \end{bmatrix} > 0 \tag{5.29}$$

and

$$\begin{bmatrix} \mathrm{L} \otimes \Lambda(R,S) + M \otimes \Phi_A + M^T \otimes \Phi_A^T & M_1^T \otimes \Phi_B & M_2^T \otimes \Phi_C^T \\ M_1 \otimes \Phi_B^T & -\gamma I & I \otimes \Phi_D^T \\ M_2 \otimes \Phi_C & I \otimes \Phi_D & -\gamma I \end{bmatrix} < 0 \tag{5.30}$$

Where

$$\Phi_A = \begin{bmatrix} AR + B\hat{C} & A + B\hat{D}C \\ \hat{A} & SA + \hat{B}C \end{bmatrix} \tag{5.31}$$

$$\Phi_B = \begin{bmatrix} B_w + B\hat{D}D_w \\ SB_w + \hat{B}D_w \end{bmatrix}$$

$$\Phi_C = [C_z R + D_z \hat{C} \quad C_z + D_z \hat{D} C]$$

$$\Phi_D = \left[D_{zw} + D_z \hat{D} D_w\right]$$

The controller that robustly put the closed-loop poles of a system in $\mathcal{D}$ is

$$K(s) = D_K + C_K(sI - A_K)^{-1}B_K$$

The matrices A_K, B_K, C_K are derived as follows.

- Compute square matrices $N$and M such that $MN^T = I - RS$.
- Solve the change of controller variables:

$$\begin{cases} \hat{C} = C_K M^T + D_K CR \\ \hat{B} = NB_K + SBD_K \\ \hat{A} = NA_K M^T + NB_K CR + SBC_K M^T + S(A + BD_K C)R. \end{cases}$$

5.3 Controller Design

- The region to put the closed loop poles is chosen as conic sector with its tip at -2
- With an angle of $\cos^{-1}(.99)$
- The poles of the closed loop function obtained is shown in the fig(5.4)

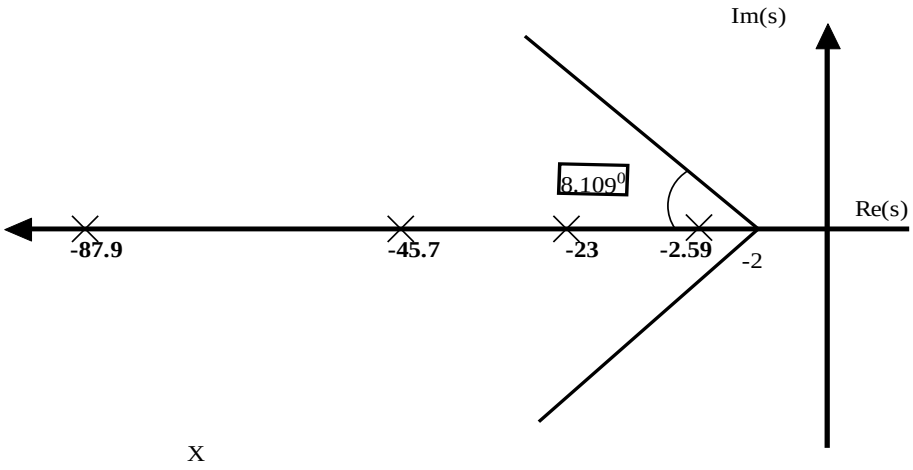

Fig 5.4 conic sector chosen for controller design

Transfer function of the controller for cart position obtained is

$$G_1(s) = \frac{.007504\,s^6 - 9393s^5 - 4.142 * 10^5 s^4 - 6.123 * 10^3 s^3 - 3.613 * 10^7 s^2 - 7.28 * 10^7 s - 3.578 * 10^7}{s^6 + 179.2s^5 + 1.078 * 10^4 s^4 + 2.767 * 10^5 s^3 + 3.206 * 10^6 s^2 + 1.587 * 10^7 s + 2.396 * 10^7}$$

Transfer function of the controller for the output pendulum angle obtained is

$$G_2(s) = \frac{.08036\,s^6 + 2.418 * 10^7 s^5 + 1.132 * 10^6 s^4 + 1.825 * 10^7 s^3 + 1.255 * 10^2 s^2 + 3.55 * 10^8 s + 3.467 * 10^8}{s^6 + 179.2 s^5 + 1.078 * 10^4 s^4 + 2.767 * 10^5 s^3 + 3.206 * 10^6 s^2 + 1.587 * 10^7 s + 2.396 * 10^7}$$

5.4 Results and Discussion

Simulations results

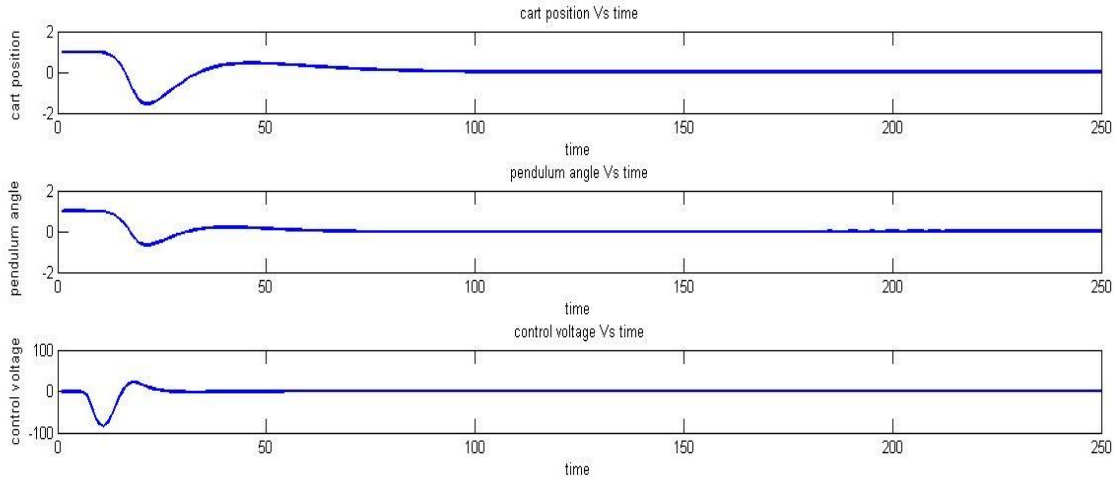

Fig 5.5: Simulation result for regional pole placement technique on IP model.

Experimental result:

The experimental results obtained for the regional pole placement technique is shown in the fig4.3. Oscillation in the cart position sustain due to unfiltered noise.

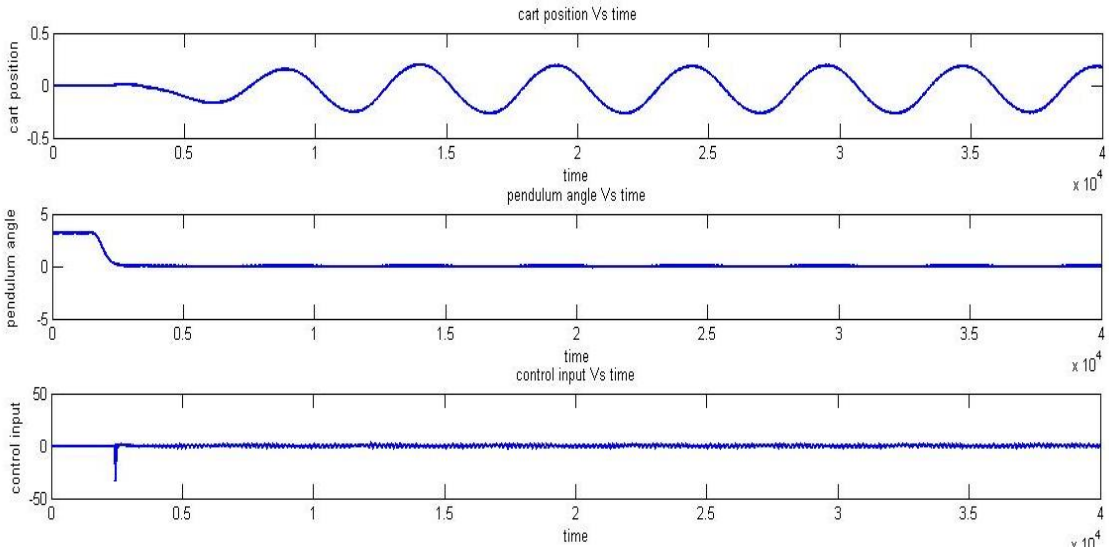

Fig 5.6: Experimental result for regional pole placement technique on IP model

5.4 Chapter summary

The chapter begins with the introduction on Regional Pole placement technique. Various LMI regions along with their characteristic equations have been specified. Controller design is being illustrated. Finally the chapter is concluded with simulation and experimental result

CHAPTER 6

6. CONCLUSION AND FUTURE WORK

6.1. Conclusions

The proposition introduces various control methodologies, for example, LQR, Two-loop PID Controller and Regional pole placement technique. These configuration routines have been fruitful in meeting the adjustment objective of the CIPS, all the while fulfilling the physical requirements in track limit furthermore, control voltage. The LQR, Two-Loop PID and RPP are effective in guaranteeing great power on the info side of the CIPS. Due to the presence of non-linear friction term in the system dynamics there has been a difficulty in obtaining the idealistic behaviour for the cart position. The Linear Quadratic Regulator (LQR) weight determination for the Cart Inverted Pendulum has been deliberately given together specific algorithm. Unlike other state feedback systems in LQR the selected weights automatically takes care of the physical constraints.

Regional pole placement technique is used and here the pole locations are chosen automatically within a specified pole region. But Continuous oscillations persists in the cart position. For a Two- Loop PID controller two loops have been used and the controller is designed based on pole placement. For Two-Loop PID controlled the oscillation in the cart position have been reduced. A Two-Loop PID controller provides a good overall performance.

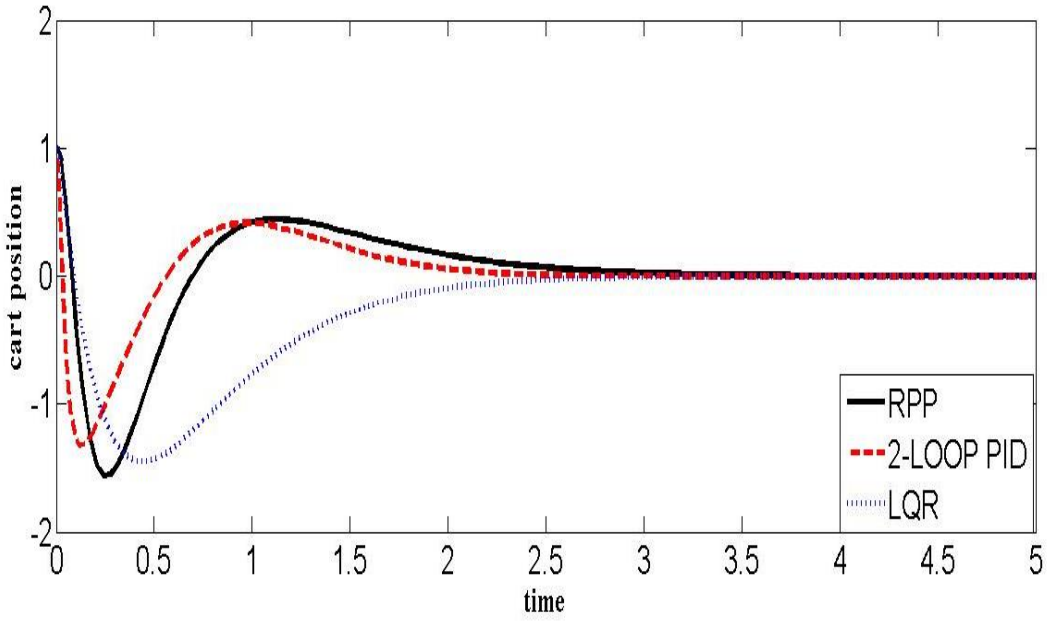

Fig6.1: Comparison of cart position for different controller

Table 6.1: Comparison of cart position for different controller

Controller	LQR	2-LOOP PID	RPP
Settling Time	2.97	2.458	2.74
Undershoot	-1.559	-1.307	-1.45
Overshoot	0.4428	0.4128	0

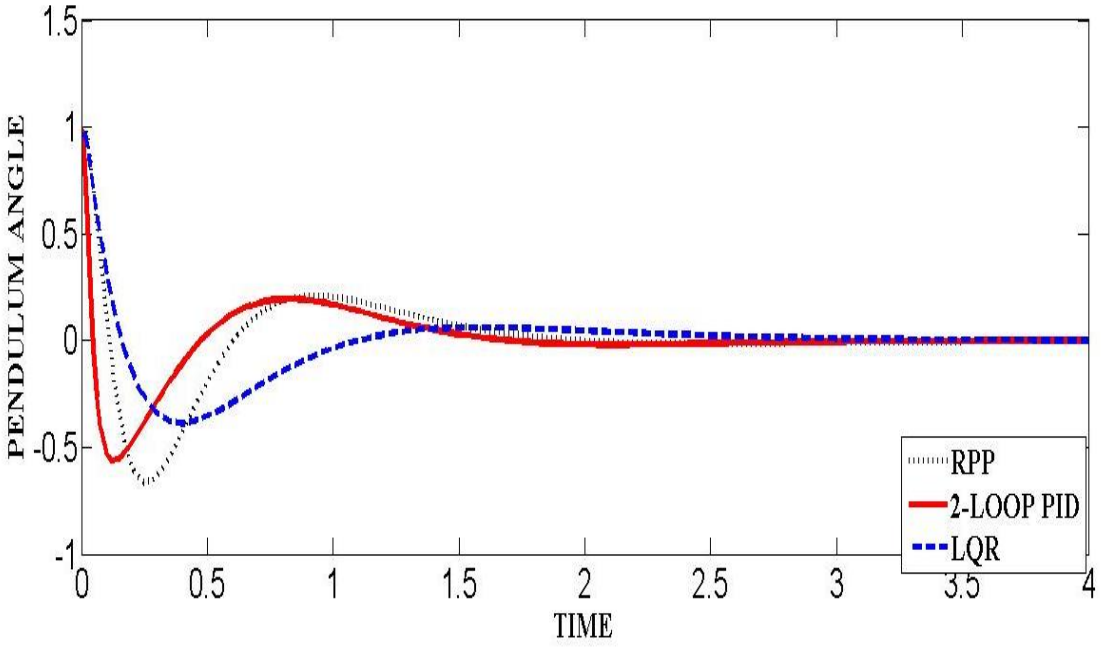

Fig6.2: comparison of pendulum angle for different controller

Table 6.2: comparison of pendulum angle for different controller

Controller	LQR	2-LOOP PID	RPP
Settling Time	1.663	1.663	2.79
Undershoot	-.564	-.6646	-.3881
Overshoot	.9	.8	0

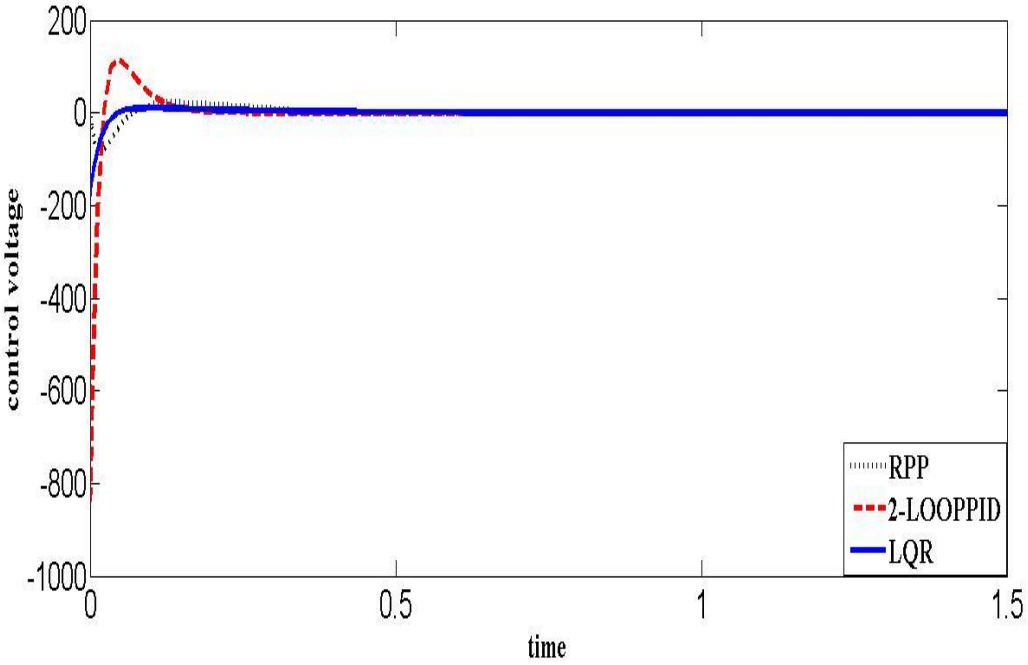

Fig6.3: comparison of control voltage for different controller

From the figures it can be observed that for LQR undershoot and overshoot are comparatively less but it takes more settling time. Settling time of the three controllers is almost same. Control voltage of 2-Loop PID is more compared to the other two controllers.

6.2. Thesis Contributions

The following are the contributions of the thesis

- A methodical calculation for weight choice for LQR has been stated
- Based on pole placement approach Two-Loop PID controller is design which leads to overall improvement of system performance
- Robust Pole placement technique has been implemented.

6.3. Suggestions for Future Work

- **Convex control method**

From the dynamics of inverted pendulum one can observe the existence of non-linear term $\sin\theta$. This non-linearity $\sin\theta$ is being linearized by using smooth mixing signals as in [18]. The paper [18] describes a convex control algorithm that can be applied on Inverted Pendulum. The design of [18] has been briefly represented below. Consider the inverted pendulum design[18]

$$\dot{\chi}_1 = \chi_2 \quad (1)$$

$$\dot{\chi}_2 = -0.1\chi_1 + \sin\chi_1 + u \quad (2)$$

Where $\chi = [\chi_1\ \chi_2]^T$ is the state of the pendulum, composed of angular position and angular velocity, and *u* is the control input torque. We are interested in applying the ConvCD technique to find a state feedback control that brings the pendulum to the upright unstable equilibrium (0,0), while minimizing the criterion

$$J = \int_0^\infty (4{\chi_1}^2(s) + 4{\chi_2}^2(s) + u^2(s))ds \quad (3)$$

A. Adding a Non-linear-Integrator: The first step in this approach is to change the dynamics of the system by adding a nonlinear integrator. The reason for adding this nonlinear integrator is that because of this addition the constraint imposed on the input is eliminated. But for this example no constrain on input is considered. A new control input 'v' is calculated as follows: $\dot{u} = v$

The augmented state vector becomes

$$x = [\chi^T\ \ u^T]^T$$

B. Approximations Using Mixing Signals: There is a nonlinear term of $\sin\theta$ in the system dynamics. To linearize that term we use five smooth mixing signals which satisfy the property inside the convex interval $-4 \le \chi_1 \le 4$

$$\beta_i(x)\epsilon[0,1],\ \sum_{i=1}^{5}\beta_i(x) = 1, \forall\, x \quad (4)$$

The interval [-4 4] is divided into L=5 overlapping subsets and five mixing signals are constructed on the basis of Gaussian function $\varphi(\chi_1, \chi_{2,}\sigma_x) = e^{-((x_1-x_0)^2/\sigma^2}$.

$$\widetilde{\beta_i}(\chi_1) = \varphi(\chi_1, \chi_{2,}\sigma_x)$$

Here x_0 is the centre of guassian function taken as [-3.2, -1.6, 0, 1.6, 3.2] and σ_x is the bell width taken as .2667. Same bell width is chosen for all signals.

In order to satisfy normalized set of mixing signals, the mixing signals $\beta_i(\chi_1)$ are generated by normalizing $\beta_i(\chi_1)\widetilde{\beta_i}(\chi_1)/\sum_{j=1}^{L}\widetilde{\beta_J}(\chi_1)$, i=1……L.

Mixing signals resulting from the procedure are shown in the figure 1

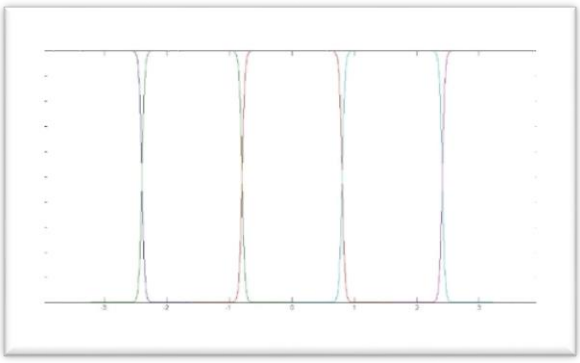

Fig1.mixing signals

$$\sin(x_1) = \beta_1(x_1).(-\theta_1 x_1 - \theta_2) + \beta_2(x_1)(-\theta_3) + \beta_3(x_1)\theta_4 x_1 + \beta_4(x_1)(\theta_3) + \beta_5(x_1).(-\theta_1 x_1 + \theta_2)$$

By using least square approximation we get the values of $\theta = [-.005\ \ -.82\ \ .97\ \ 1]$.

After PWL approximation the system will be in the form of

$$\dot{x} = \sum_{i=1}^{L}\beta_i(x)(A_i\bar{x}(x) + Bv) \quad (5)$$

Where $\bar{x}(x) = [\chi_1\ \ \chi_2\ \ 1\ u]^T$

$$B = [0\ 0\ 0\ 1]^T$$

$$A1 = \begin{bmatrix} 0 & 1 & 0 & 0 \\ .005 & -.1 & .82 & 1 \\ 0 & 0 & 0 & 0 \\ 0 & 0 & 0 & 0 \end{bmatrix} \quad A2 = \begin{bmatrix} 0 & 1 & 0 & 0 \\ 0 & -.1 & -.97 & 1 \\ 0 & 0 & 0 & 0 \\ 0 & 0 & 0 & 0 \end{bmatrix} \quad A3 = \begin{bmatrix} 0 & 1 & 0 & 0 \\ 1 & -.1 & 0 & 1 \\ 0 & 0 & 0 & 0 \\ 0 & 0 & 0 & 0 \end{bmatrix}$$

$$A4 = \begin{bmatrix} 0 & 1 & 0 & 0 \\ 0 & -.1 & .97 & 1 \\ 0 & 0 & 0 & 0 \\ 0 & 0 & 0 & 0 \end{bmatrix} \quad A5 = \begin{bmatrix} 0 & 1 & 0 & 0 \\ -.005 & -.1 & -.82 & 1 \\ 0 & 0 & 0 & 0 \\ 0 & 0 & 0 & 0 \end{bmatrix} \tag{6}$$

The state equation now will be in the form of: $\dot{x} \approx \overline{\emptyset}(x)z(x) + Bv$ (7)

$$\overline{\emptyset}(x) = \left[\sqrt{\beta_1(x)}A1 \quad \cdot \quad \cdot \quad \sqrt{\beta_2(x)}AL\right]$$

And the vector z(x) is defined as follows $z(x) = \begin{bmatrix} \sqrt{\beta_1(x)}\bar{x}(x) \\ . \\ . \\ . \\ \sqrt{\beta_L(x)}\bar{x}(x) \end{bmatrix}$ (8)

C. Controller Approximations: By applying the above transformations, the optimal state feedback design problem will be

$$\text{Minimise } J = \int_0^\infty (z^T(s)Qz(s))ds \tag{10}$$

$$\text{Subjected to } \dot{x} = \overline{\emptyset}(x)z(x) + Bv + B\Gamma(x)G \tag{11}$$

C (ii). Application of HJB equation:

For a system $\dot{x}(t) = f(x(t), u(t), t)$
With PI as

$$J(x(t_0), t) = \int_{t_0}^{t_f} V(x(t), u(t), t)dt.$$

Now we obtain the control law as a function of state variables, leading to closed loop optimal control.

A scalar function $J^*(x^*(t), t) = \int_t^{t_f} V(x^*(\tau), u^*(\tau), \tau)d\tau$

$$\frac{dJ^*(x^*(t), t)}{dt} = \left(\frac{\partial J^*(x^*(t), t)}{\partial x^*}\right)' \dot{x}^*(t) + \frac{\partial J^*(x^*(t), t)}{\partial t},$$

$$= \left(\frac{\partial J^*(x^*(t), t)}{\partial x^*}\right)' f(x^*(t), u^*(t), t) + \frac{\partial J^*(x^*(t), t)}{\partial t}$$

$$\frac{dJ^*(x^*(t), t)}{dt} = -V(x^*(t), u^*(t), t)$$

$$\frac{\partial J^*(x^*(t), t)}{\partial t} + V(x^*(t), u^*(t), t) + \left(\frac{\partial J^*(x^*(t), t)}{\partial x^*}\right)' f(x^*(t), u^*(t), t) = 0$$

Let us introduce Hamiltonian

$$\mathcal{H} = V(x^*(t), u^*(t), t) + \left(\frac{\partial J^*(x^*(t), t)}{\partial x^*}\right)' f(x^*(t), u^*(t), t)$$

Substituting the value of $\mathcal{H}$ in the above equation

$$\frac{\partial J^*(x^*(t),t)}{\partial t} + \mathcal{H}\left(x^*(t), \frac{\partial J^*(x^*(t),t)}{\partial t}, u^*(t), t\right) = 0 \quad \forall t \in [t_0 t_f)$$

From boundary conditions we get

$J^*\left(x^*(t_0), t_f\right),)$=0

Costate function is given by

$$\lambda^*(t) = \frac{\partial J^*(x^*(t),t)}{\partial x^*}$$

State and costate function are related by

$$\dot{\lambda}^*(t) = -\left(\frac{\partial \mathcal{H}}{\partial x}\right)$$

Optimal control u is obtained from $\left(\frac{\partial \mathcal{H}}{\partial x}\right) = 0$

$$u^*(t) = h(x^*(t), J_x{}^*, t)$$

Comparing above two equations we get $\frac{d}{dt}\left(\frac{\partial J^*(x^*(t),t)}{\partial x^*}\right) = \frac{d}{dt}[\lambda^*(t)]$

$$= -\frac{\partial \mathcal{H}\left(x^*(t), \frac{\partial J^*(x^*(t),t)}{\partial t}, u^*(t), t\right)}{\partial x^*}$$

Using $J_t^* = \frac{\partial J^*(x^*(t),t)}{\partial t}$ and $J_x^* = \frac{\partial J^*(x^*(t),t)}{\partial t}\frac{\partial J^*(x^*(t),t)}{\partial t}$

HJB equation becomes

$$\boldsymbol{J_t^* + \mathcal{H}(x^*(t), J_x^*, u^*(t), t)=0}$$

Application of the Hamilton–Jacobi–Bellman (HJB) equation to the above problem results in the following:

$$-z^T Q z = \frac{\partial V^T}{\partial x}(x)\left(\bar{\emptyset}(x)z(x) + Bv^* + v\right)ds \tag{12}$$

V is optimal cost to go function.

The optimal cost-to-go function V is a controlled lyapunov function (CLF).

The CLF can be approximated using piece wise approximation of lyapunov function as follows:

$$V(x) \approx \sum_{i=1}^{L} \beta_i(x)\bar{x}(x)P_i\,\bar{x}(x) = z^T(x)Pz(x) \tag{13}$$

Where P is a positive semi-definite matrix.

Similar to the approximations for optimal cost to go function V, the optimal controller function can be approximated as

$$v^* \approx \sum_{i=1}^{L} \beta_i(x)\,G_i z(x) = \Gamma(x)gz(x) \tag{15}$$

Where G_i are constant matrices.

D. THE CONVCD APPROACH:

Using approximation (13), (15) the HJB can be represented as

$$0 = z^T([\bar{\emptyset}(x) + B\Gamma(x)G]^T M_z^T P + PM_z\left[\bar{\emptyset}(x) + B\Gamma(x)G\right] + Q)z - \bar{v} \tag{16}$$

$$0 = \mathcal{G}_{P,G}(x) - \bar{v}$$

For closed loop stability we have $\dot{V} < 0\ for\ x \neq 0\ or\ if$

The following inequality holds:

$$\mathcal{L}_{P,G} \approx z^T([\overline{\emptyset}(x) + B\Gamma(x)G]^T M_z^T P + PM_z\left[\overline{\emptyset}(x) + B\Gamma(x)G\right])z < 0 \; \forall x \notin \mathcal{B}(\bar{v}) \tag{17}$$

Equations (16) and (17) indicate that it suffices to choose **P**,**G** so that the term $\mathcal{G}_{P,G}(x)$ is as small as possible subject to the constraint $\mathcal{L}_{P,G}$ that is—almost—negative definite. In other words, the problem of constructing an approximately optimal performance can be cast as the following optimization problem:

$$min\left\|\mathcal{G}_{P,G}(x)\right\|^2 + \gamma$$

S.T P > 0

$$\mathcal{L}_{P,G} \leq -\gamma, \gamma > c > 0, \forall x \notin \mathcal{B}(\bar{v}) \tag{18}$$

The above problem is nonlinear with respect to P,G. So solving a non-convex problem is hard so we transform it into convex by multiplying terms inside the parenthesis by P^{-1}

$$\mathcal{F}_{\bar{P}F\bar{Q}}(x) \triangleq z^T([P\overline{\emptyset}(x) + B\Gamma(x)F]^T M_z^T + M_z\left[\overline{\emptyset}(x)P + B\Gamma(x)F\right] + Q)z$$

$$= \bar{\bar{v}} \tag{19}$$

$$\bar{P} \triangleq P^{-1}, \bar{Q} \triangleq \bar{P}Q\bar{P} = P^{-1}QP^{-1} \tag{20}$$

F is a matrix satisfying

$$F=G\bar{P}$$

$$\mathcal{H}_{\bar{P}F} \triangleq z^T\left(\left[P\overline{\emptyset}(x)^T + F^T\Gamma(x)B^T\right]M_z^T + M_z\left[\overline{\emptyset}(x)P + B\Gamma(x)F\right]\right)z < 0, \forall x \notin \mathcal{B}(\bar{v}) \tag{22}$$

The above two equations are so the problem statement now will be

$$\text{Minimise } \gamma_1 + \gamma_2$$

S.T constraints:

$$\gamma_2 I - F^T F \geq 0$$

$$\epsilon_1 I \leq \bar{P} \leq \epsilon_2 I$$

$$\epsilon_3 Q \leq \bar{Q}$$

$$\mathcal{H}_{\bar{P}F}(x) \leq -\gamma_1,$$

$$\gamma_1 > c > 0,$$

$$\gamma_2 > c > 0 \quad \forall x \notin \mathcal{B}(\bar{v}) \tag{23}$$

Since the optimisation problem here is infinite dimension and state dependent problem we discretise the state space. The number of discretization points does not have to be as large.

$$\text{Minimise } \gamma_1 + \gamma_2$$

S.T constraints

$$\sum_{i=1}^{N} \mathcal{F}_{\bar{P}F\bar{Q}}\left\|(x^{[i]})^2\right\|^2 \leq \gamma_2$$

$$\epsilon_1 I \leq \bar{P} \leq \epsilon_2 I$$

$$\epsilon_3 Q \leq \bar{Q}$$

$$\mathcal{H}_{\bar{P}F}\left(x^i\right) \leq -\gamma_1,$$

$$\gamma_1 > c > 0,$$

$$\gamma_2 > c > 0 \quad \forall x \notin \mathcal{B}(\bar{v}) \tag{24}$$

The ConvCD algorithm (24) is run with $N = 6, \epsilon_1$=1,$\epsilon_2 = 20, \epsilon_3 = 1\ L = 5$.

The above problem is solved by using LMI and the controller thus obtained is applied to the plant. And the states are observed. The cost function is to be minimised.

But in the above problem the LMI is made to run for a minimum of 250 iterations. Which takes a lot of time.

- Other Control methods like Integral Slide Mode controller, fuzzy control etc. may be attempted.

7. REFERENCES

[1] K.J.Aström, and R.M.Murray, "Feedback systems: an introduction for scientists and engineers." Princeton university press, 2010.

[2] "Digital Pendulum: Installation and Commissioning Manual", East Sussex, U K: Feedback Instruments Ltd., 2007.

[3] "Digital Pendulum: Control Experiments Manual", East Sussex, U K: Feedback Instruments Ltd., 2007.

[4] "Getting Started with Real-Time Workshop ver. 5", M A: The MathWorks Inc., July 2002.

[5] S. H. Zak, "*Systems and Control*", N Y: Oxford University Press, 2003.

[6] O.Boubaker, "The inverted pendulum: A fundamental benchmark in control theory and robotics," *Education and e-Learning Innovations (ICEELI), 2012 International Conference on*, vol., no., pp.1,6, 1-3 July 2012

[7] W.Li; H.Ding; K.Cheng, "An investigation on the design and performance assessment of double-PID and LQR controllers for the inverted pendulum," *Control (CONTROL), 2012 UKACC International Conference on*, vol., no., pp.190, 196, 3-5 Sept. 2012

[8] E. Vinodh Kumar, J.Jerome, Robust LQR Controller Design for Stabilizing and Trajectory Tracking of Inverted Pendulum, *Procedia Engineering*, Volume 64, 2013, Pages 169-178, ISSN 1877-7058

[9] A Roshdy, Amr, Hany F Mokbel, and W.Tongyu. "Stabilization of Real Inverted Pendulum Using Pole Separation Factor." *Proceedings of the 1st International Conference on Mechanical Engineering and Material Science*. Atlantis Press, 2012.

[10] M. W. Dunnigan, "Enhancing state-space control teaching with a computer-based assignment," *IEEE Transactions on Education*, vol.44, no.2, pp.129-136, May 2001

[11] P.Cominos, and N. Munro. "PID controllers: recent tuning methods and design to specification." *IEE Proceedings-Control Theory and Applications* 149.1 (2002): 46-53.

[12] M.Chilali, P. Gahinet, and P.Apkarian. "Robust pole placement in LMI regions." *Automatic Control, IEEE Transactions on* 44.12 (1999): 2257-2270.

[13] Gutman, Shaul, and E.Jury. "A general theory for matrix root-clustering in sub regions of the complex plane." *Automatic Control, IEEE Transactions on* 26.4 (1981): 853-863.

[14] A.Ghosh.; T.R Krishnan, B.Subudhi., "Robust proportional- integral-derivative compensation of an inverted cart-pendulum system: an experimental study," *Control Theory & Applications, IET*, vol.6, no.8, pp.1145,1152, May 17 2012

[15] T. R. Krishman, "On Stabilization of Cart-Inverted Pendulum System: An Experimental Study", Master of Technology thesis NIT Rourkela,2013.

[16] S. Boyd, L. E. Ghaoui, E. Feron, V. Balakrishnan, 'Linear Matrix Inequalities in System and Control Theory,' Philadelphia , Pennsylvania: SIAM, 1994

[17] 'LMI Control Toolbox' by Pascal Gahinet Arkadi Nemirovski , Alan J. Laub ,M.Chilali

[18] S. Baldi, I.Michailidis, E.B. Kosmatopoulos, A.Papachristodoulou, and P.A.Ioannou "Convex Design Control for Practical Nonlinear Systems", *IEEE Transactions on Automatic Control, VOL. 59, NO. 7, JULY 2014*

[19] A. Rantzer and M. Johansson, "Piecewise linear quadratic optimal control", *IEEE Trans. Automatic Control, vol. 45, pp. 629–637, 2000.*

[20] S. Skogestad and I. Postlethwaite, '*Multivariable Feedback Control: Analysis and design*,' 2nd Edition, Chichester, John Wiley and Sons, 2005.